

We thank both anonymous reviewers for their timely comments. Their comments are reproduced in black text and our responses are in blue text. Text added directly to the manuscript is *indented and italicized* or pasted via screenshot. Please see the tracked changes version as well.

Anonymous Referee #1

Received and published: 13 August 2017

This study presented interesting results on how inorganic-organic interactions would influence particle partitioning, based on observation and simulation results from several models. Generally, this paper is comprehensive and well organized, while several concerns should be addressed before publishing.

Major Comments:

(1) In section 3.1, the authors attributed the discrepancy between CMAQ and observations to the inappropriate inclusion of cations from insoluble metal oxides. They further indicated that the overestimation of transition metals could not be avoided even if the dust emissions are closed. However, they did not state clearly whether the dust emissions were closed in their simulations, and to what extent that would make a difference. In fact, as shown in Fig. 2, CMAQ substantially underestimated ammonia F_p , while the RN/2S are comparable with other models. Does that arise from the overestimated total ammonia emissions, or more from the overestimated non-volatile cations that would bias the aerosol acidity and therefore the gas-particle partitioning? These mechanisms should be better described and quantified.

Appel et al. (2013) conducted simulations in which wind-blown dust emissions were removed from CMAQ to evaluate the effect on cation predictions. We include dust emissions following Foroutan et al. (2017) as indicated in section 2.1, and we did not repeat the sensitivity simulation of removing wind-blown dust by Appel et al. in this work. However, in response to comments from both reviewers we conducted an additional sensitivity simulation in which all nonvolatile cations (Na, K, Mg, Ca) were removed from the ISORROPIA thermodynamic calculations in CMAQ for fine aerosol. The sensitivity simulation results in RN/2S values of 1 for the eastern US demonstrating that cations cause the low RN/2S in CMAQ:

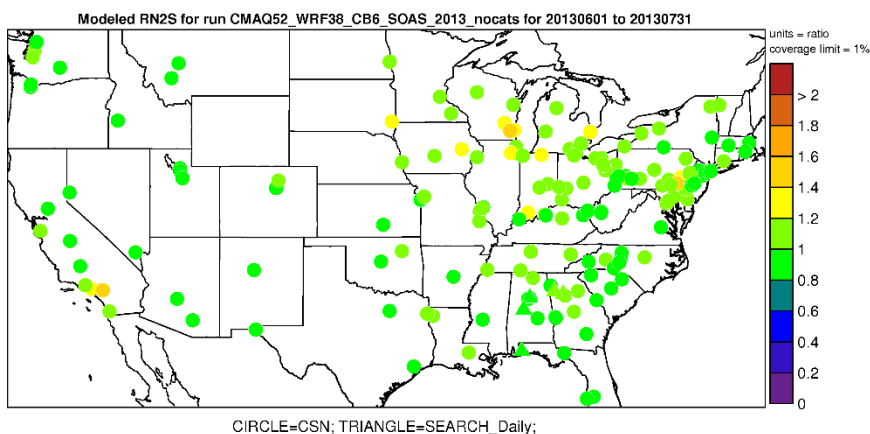


Figure AC1: Ratio of ammonium to 2 x sulfate predicted in a CMAQ simulation without nonvolatile cations (1 June – 15 July 2013). The model is sampled at CSN (circle) and SEARCH (triangle) locations.

Furthermore, we quantify the overestimate in nonvolatile cations in a new table in the SI and add text to the manuscript indicating the factor of 3 overestimate in nonvolatile cations. If the excess cations were corrected and replaced by ammonium, it would lead to a 26% increase in ammonium.

Revised text (abstract):

were consistent with these conditions. CMAQv5.2 regional chemical transport model predictions did not reflect these conditions due ~~to biases in a factor of three overestimate of the nonvolatile cations that resulted from either overestimated emissions~~

Revised text (section 3.1):

An overabundance of cations in the CMAQ model (Figure S1, Table S10) means that ammonium was displaced from the particle and RN/2S was biased low for the southeast U.S. An evaluation of the individual cations and anions (Figure S1, Table S10) indicated CMAQ over predicted the non-volatile ISORROPIA cations (Na⁺, Ca²⁺, K⁺, Mg²⁺) by factors of 2 to 6 individually and by a charge equivalent factor of 3 overall in the Southeast. A factor of 3 overestimate in nonvolatile cations indicates ammonium predicted by CMAQ was low by about 26%.

A sensitivity simulation in which all Aitken and accumulation mode Na⁺, Ca²⁺, K⁺, and Mg²⁺ were removed from the partitioning thermodynamics resulted in a mean predicted RN/2S of 0.96 for the southeast U.S.

Underestimates in ammonia Fp are due to both the replacement of NH₄⁺ by nonvolatile cations and to overestimates in NH₃ emissions (both operate in the same direction). Note that during SOAS total NH₃ was significantly overestimated in CMAQ (Figure S8) and removing the cations only increases NH_x Fp slightly (revised Figure 2g,h). Overestimates in NH₃ would not cause low RN/2S.

A new boxplot “CMAQ, no cations” was added to Figure 2. Revised text:

Note that in full CMAQ model calculations, the predicted nonvolatile cation concentrations were so high that they erroneously affected the partitioning of ammonium (Table S10, Figure S1). Removing nonvolatile cations from CMAQ (h) allowed more ammonium into the particle and led to increased RN/2S, but NH_x Fp was still low indicating overestimates in gas-phase ammonia in the CMAQ model are not primarily due to the displacement of ammonium by nonvolatile cations.

(2) In section 3.1, the different RN/2S ratios from CSN and SEARCH networks are attributed to measurement errors. However, the discrepancy is over 33%, which cannot be totally explained by the <20% measurement errors from Nylon filter. Other possible error sources should be discussed, and the influence of the observation uncertainty should also be discussed in subsequent sections.

Section 3.1 highlights some known instances of measurement bias which include: SO₂ collection on nylon filters and NH₄ volatilization from nylon filters. From Solomon et al.’s description of the IMPROVE and CSN networks: “Overall measurement accuracy is not possible for most PM measurements since

traceable standards applied in the field are not available.” We have added the CSN and SEARCH measurement precision, which is much less than the difference in measurement techniques, to section 2.2:

Solomon et al. (2014) estimate the precision of CSN measured ammonium is 11% and sulfate is 7% (for co-located samples during 2012) but the actual measurement uncertainty is likely higher (and not quantified).

SEARCH reports the precision of measured sulfate and ammonium in PM_{2.5} is 2-3% (Edgerton et al., 2005).

Section 3.2 has also been revised to include a discussion of AMS uncertainty. Revised text:

The differences in the AMS and MARGA datasets in terms of RN/2S are larger than can be explained by known measurement precision. However, uncertainty for AMS measured ammonium (34%) and sulfate (36%) are large (Bahreini et al., 2009). A contributor to this uncertainty is the AMS collection efficiency (CE), and AMS instruments ...

(3) In section 3.4, when phase separation occurred, what is the acidity of each phase?

In a liquid-liquid phase separation case for AIOMFAC EQLB predictions, each phase had a similar pH. The predictions show a typical absolute difference of less than 0.2 pH units (frequently less than 0.1 pH units), i.e. clearly within the range of variability of the values reported in Table 1. The difference is small since liquid-liquid equilibrium thermodynamics drive activity-based pH values to have nearly the same magnitude in coexisting phases (but not necessarily exactly the same values). A sentence in section 3.3 was revised to add the H⁺ air value from Figure 3 to the text.

The β phase, with its higher concentration of organic species, showed a lower average [H⁺]_{air} (0.1 nmol/m³) compared to the α phase (1.5 nmol/m³), while the activity-based pH values were predicted to be similar in both phases, typically within 0.2 pH units (as expected from equilibrium thermodynamics).

(4) In section 3.4, the authors claimed that all the high-pH points are due to measurement uncertainty, which is not convincing. Does these points all occur at very low concentrations when the uncertainty is extremely large? Moreover, they mentioned that there were some elevated nitrite episodes, probably from sea-salts. Whether the high-pH points correspond with those episodes should be examined.

pH=7 predictions are not restricted to low concentrations (Figure AC2, left) or high NaCl concentrations. They are associated, by design, with an excess of cations compared to anions (Figure AC2, right). This is the case in the AIOMFAC-based calculations because the presence of charge-weighted excess amounts of cations in the measured ion concentration data meant that no explicit amount of H⁺ was necessary to establish a neutral charge in the overall aerosol mixture (nor was HSO₄⁻ quantified among the measured anions). Note that the H⁺ concentration was not measured, but inferred via an overall charge balance constraint in cases with an excess of anions (excess negative charge) to initialize the model calculations with AIOMFAC. Therefore, by default, the pH value was set to 7 in cases where no H⁺ ions were present in the mixture at input (autodissociation of water is not explicitly considered). Since an excess in positive charge may occur erroneously as the result of measurement uncertainties during cation and anion

quantification, it remains possible that the particles with a reported pH of 7 were in fact acidic. This hints to the challenges in accurate H^+ concentration quantification in the field and related sensitivities in predicted particle pH. A small decrease in the cation abundance, as demonstrated by Hennigan et al. (2015) can lead to a significantly lower pH. Figure AC2 (right) shows that pH=7 is obtained when the cations meet or exceed the anions.

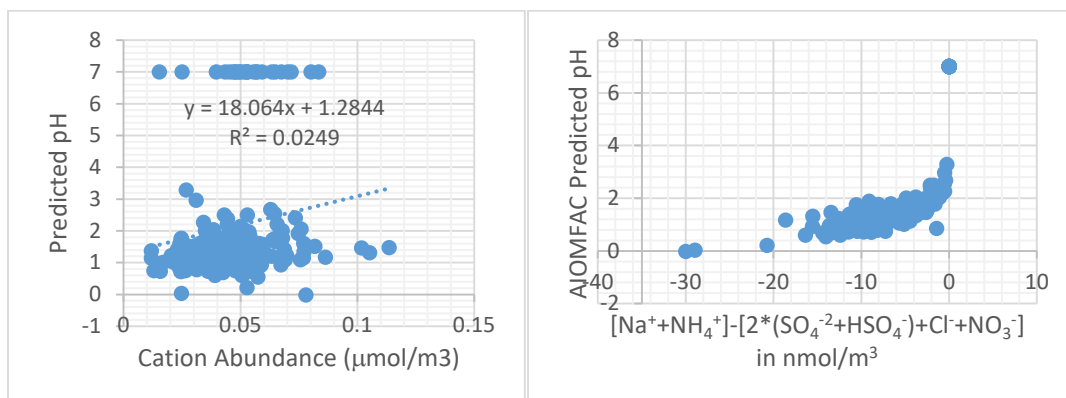


Figure AC2: (left) Predicted pH vs. molar cation abundance (ammonium+sodium+hydronium) used in AIOMFAC calculations. (right) Predicted pH vs cations-anions.

(5) The implication of results shown in this study, and future work directions should be discussed more in-depth. For example, what is the major strength and weakness of current models shown in this study? Should the second organic phase of, say, HOAs, as mentioned in section 3.5, be added in the future?

As HOA was not resolved in the AMS PMF analysis, it likely contributed <5% of total organic aerosol. A third liquid phase could be examined as part of future work.

We have added this additional text to the conclusions to emphasize our main message (also in response to the Weber et al. comment in ACPD):

The lack of agreement of AMS and CSN data with thermodynamic models, but the agreement between MARGA observations and models, indicates a potential bias in CSN measurements and that AMS data alone may not be suitable for thermodynamic modeling. The diversity in observational datasets can explain why some work has concluded thermodynamic models fail (Silvern et al., 2017) while others indicate models are adequate (Weber et al., 2016). This work finds thermodynamic...

To highlight the strength of the AIOMFAC-based model, we add in Section 3.2:

Comparing the change in mean NH_x Fp with (m) and without (l) organic compound interactions indicates that organic compounds have a larger effect on ammonia gas-particle partitioning than the inclusion (j) or lack (k) of calcium, potassium, magnesium, sodium, nitrate, and chloride.

Minor points:

(1) In Figure 1, the colors of 0.8~1 and 1.0~1.2 are hardly distinguishable. If this is not on purpose, please change the colormap. Also consider adding 2 panels showing the

difference between observed and modeled RN/2S and R+/-.

We have changed the color bar. A new table, Table S10, provides CMAQ model performance metrics vs CSN and SEARCH for all cations and anions involved in ISORROPIA calculations.

(2) The relationship of IMPROVE and SEARCH network should be clarified or unified. All through the manuscript the "SEARCH" network is referred to, while in Fig. S1 to S5 "IMPROVE" is used.

SEARCH and IMPROVE are different networks. The IMPROVE network data does not appear in the main manuscript since it does not measure ammonium. We added the following to section 2.3:

The Interagency Monitoring of Protected Visual Environments (IMPROVE) network (Solomon et al. 2014) also measures some chemical speciation of PM_{2.5} throughout the U.S., but does not include ammonium.

The SEARCH network operates at fewer sites and exclusively in the Southeast U.S.

Anonymous Referee #2

Received and published: 14 August 2017

General Comments

This study examines the partitioning of inorganic and organic species in the southeast US summer using information from a large number of observational data sets and explores several different modeling frameworks to describe the partitioning of these species with varied levels of sophistication and agreement with observations. The inclusion of organics and phase separation as well as the organic compound composition is shown to be important for determining aerosol acidity and ammonia partitioning. This work is an important contribution to the modeling community's treatment of inorganic and organic aerosol species. The paper is well written and highly detailed, and below are specific comments to be considered in the revision of this manuscript.

Specific Comments

Page 3, lines 1-3: NAAQS are set for certain particulate precursors (SO₂, NO₂), so is the reference specifically to NH₃ and organic gases?

Yes. (NH₃ and organic compound vapors) has been added.

Page 3, line 18: Please cite NEI version used in CMAQ simulations and clarify "specific when available."

2011 National Emission Inventory version 2 is already indicated, but we have added "ek" as further identification. We also revised "specific when available" to:

Emissions influenced by model meteorology (biogenic compounds, mobile sector) or monitored (electrical generation units) were year 2013 specific.

Page 3, lines 27-29: It would be helpful for the authors to distinguish between the use

of forward and reverse modes of ISORROPIA for clarity and consistency with thermodynamic modeling literature.

Forward and reverse mode definitions have been added to the text in section 2.1.

Section 2.2: How do the AMS measurements used in this study compare to the other AMS measurements made at the same site during the measurement campaign (Hu et al., 2015), which do include nitrate (and chloride). How do SOAS measurements compare with SENEX and SEAC4RS measurements?

An examination of SENEX data is beyond the scope of our paper, but has been modeled in previous work. All of the AMS measurements from SOAS and SEAC4RS are similar. Table S5 shows a comparison of SOAS-CTR measurements while table S6 summarizes results from SEAC4RS and the work of Silvern et al (2017). All AMS data indicate average ratios of ammonium to 2*sulfate of 0.6 or lower. Nitrate measured by the AMS includes both inorganic (able to participate in inorganic aerosol thermodynamics) and organic (Xu et al. 2015b) compounds. Thus we do not consider nitrate in our AMS-based thermodynamic calculations since the fraction that is inorganic is not precisely known. Running ISORROPIA with and without Ca, K, Mg, Na, Cl, and NO₃ from MARGA (Figure 2i,j) indicates they are not present in enough abundance to significantly change ammonium to sulfate ratios or the fraction of NH_x in the particle (i.e. the ratios change by less than 0.1). Added to section 2.2:

This AMS dataset was consistent with the other AMS instrument operating at CTR as well as AMS measurements aboard an aircraft over the southeastern U.S. (Table S5-S6).

Page 5, line 32–page 6, line 1: Clarify the trigger condition; what is the ammonium associated with if $\text{NH}_4^+ \geq 2 \times \text{SO}_4^{2-}$?

Measured concentrations have uncertainty and thus $\text{NH}_4^+ \geq 2 \times \text{SO}_4^{2-}$ could represent unrealistic conditions. Minor amounts of NH₄ could be associated with Cl or NO₃. The reason for introducing bisulfate is a technical one; it is done since for a H⁺ and bisulfate-free electrolyte input, i.e. only (NH₄)₂SO₄ at input (no NH₄HSO₄ nor H₂SO₄), no explicit acidity nor partial association of H⁺ and SO₄²⁻ to HSO₄⁻ are considered by the AIOMFAC model. Therefore, such an input would always lead to a neutral (pH = 7) solution. However, the addition of a tiny amount of NH₄HSO₄ triggers the bisulfate dissociation equilibrium calculation and the pertaining acidity and pH-dependent ammonia gas-particle partitioning under given conditions. The additional AIOMFAC-based partitioning calculations using all anion amounts (Cl, NO₃, SO₄, NH₄, equivalent Na) did not perform the resetting of mass (i.e. introduction of bisulfate). We clarified that the introduction of bisulfate was performed for MARGA sulfate-ammonium (A') inputs only. Since AMS data never met this condition, the location of the sentence was also moved to after the MARGA data was introduced and additional text added:

The data from MARGA was used in two ways for model calculations with AIOMFAC. (1) All the measured ion concentrations were considered, but the molar amounts of the cations Ca²⁺, K⁺, Mg²⁺, and Na⁺ were mapped to a charge-equivalent amount of Na⁺ (see Section 2.1). (2) Only the measured concentrations of ammonium and sulfate ions were considered and mapped to the electrolyte components ammonium sulfate, ammonium bisulfate, and sulfuric acid for AIOMFAC model input purposes. For ammonium-sulfate only conditions (option 2) in which the moles $\text{NH}_4^+ > 2 \times \text{SO}_4^{2-}$, a small amount ($1 \times 10^{-4} \mu\text{g m}^{-3}$) of ammonium bisulfate was added to the AIOMFAC input for MARGA calculations in order to trigger a potential partial association of

sulfate and H⁺ ions to bisulfate following the equilibrium constant of that reaction. *Such conditions did not occur with AMS data.*

Section 2.2 SEARCH ammonia observations: Are these measurements hourly or 24-hr averages and are they only coincident with SOAS AMS observations? Are the measurements sensitive to diurnal variations and possible measurement interferences at cold temperatures/low relative humidity?

Box model calculations use hourly inputs of ammonia. Very low RH and cold temperatures were likely not experienced during summer at SOAS. We add:

Hourly Gas-phase ammonia was obtained from the CTR SEARCH network site via a corrected Thermo Scientific citric acid-impregnated denuder.

Section 3.1: It would be helpful to include a discussion of model biases in ammonium and sulfate, even if RN/2S is okay. Why is there a disagreement in the model bias between IMPROVE and CSN sites for sulfate? Is sea salt sulfate an important contributor to total sulfate in the model and observations along the coasts?

We do not specifically examine the role of sea salt mediated sulfate or sites on the coast, but that topic has been examined in other work (Kelly et al., 2010 GMD <https://www.geosci-model-dev.net/3/257/2010/> for example). Na and Cl are not major drivers of ammonium to sulfate ratios as indicated by sensitivity simulations conducted with and without Na, Cl, K, Mg, Ca, and NO₃ for SOAS.

IMPROVE sites specifically target Class I areas such as National Parks and Wilderness areas. The overestimate in CMAQ-predicted sulfate compared to CSN, but underestimate compared to IMPROVE could indicate a bias as a function of photochemical age in the model, but sulfate is relatively unbiased overall (normalized mean bias of 5% compared to CSN and -12% compared to SEARCH in the Southeast, Table S10). New text added:

CMAQ-predicted sulfate was relatively unbiased in the southeastern U.S. (normalized mean bias of 5% compared to CSN), but ammonium was high by a factor of 1.5 (Table S10).

We have refocused the supporting information on sulfate and ammonium as well as CSN and SEARCH: Figure 1b was eliminated since the Central US is not a focus of the study. Figure S4 showing the nitrate bias has been eliminated since nitrate is not a major constituent affecting inorganic PM in the southeast US in summer. Figure S5 was eliminated. The main goal of Figure S5 was to show ammonium and sulfate which is contained in other plots. Figure S2-S3: The included data sets have been expanded to include the SEARCH network.

A table of model performance for ammonium and sulfate (as well as other species) has been added (Table S10). For additional evaluation of sulfate and ammonium during other seasons and across the U.S., we refer the reader to Appel et al. 2017 (<https://www.geosci-model-dev.net/10/1703/2017/gmd-10-1703-2017.pdf>).

Section 3.1: It is unclear why Na, Ca, K, and Mg used in ISORROPIA's calculations in CMAQ shouldn't be. If the problem is that their concentrations in CMAQ are overesti

mated as is pointed out in the text, what can be done? It is a concerning conclusion to draw that CMAQ can't be used to diagnose species partitioning.

CMAQ still provides valuable information and we demonstrate via box modeling that if the nonvolatile cation abundance can be corrected, the thermodynamics based on ISORROPIA should operate consistently with how MARGA and SEARCH observations indicate the system should behave. We now include an estimate of the cation overabundance (factor of 3 overall, factor of 2-6 for individual cations, Table S10) as a benchmark for resolving emission issues.

We also add:

By performing ISORROPIA and AIOMFAC box modeling, this work demonstrates that our current thermodynamic understanding of ammonium and sulfate aerosol is consistent with (MARGA) observations in the southeastern U.S. atmosphere. Since models like CMAQ use the same thermodynamic basis, specifically ISORROPIA, these results build confidence that regional models can capture the thermodynamics of the ambient atmosphere. However, our results also demonstrate that for the partitioning of ammonia and ammonium to be correct, errors in emissions of nonvolatile cations, on the order of a factor of 3, must be resolved as well.

Figures S2-S4: It would be helpful to add SEARCH observations to these plots as a supplement to the ratios shown in Figure 1.

Added

Page 7, lines 22-23: Why a 10% overestimate in sulfate if in line 16 there is a 4-5% overestimate cited?

The 4-5% overestimate was due to SO₂ uptake onto filters in studies from the 1990s; as stated in the manuscript, it refers to 4 – 5 % uptake of gas phase SO₂ onto nylon filters, which is not to be interpreted as a 4 – 5 % overestimate in particulate sulfate. We do not know the magnitude of the particulate sulfate artifact for conditions in the current SE US. We point out that only a 10 % overestimate in sulfate combined with a 10 % underestimate in NH₄ could have the order of magnitude effects on RN/2S that we observe.

Page 7, line 31-page 8, line 1: Why is NH_x Fp so similar and RN/2S very different between the two ISORROPIA runs?

This comment refers to ISORROPIA simulation of AMS data using aerosol-only (forced to reproduce RN/2S) or gas + aerosol inputs (RN/2S is output). If the observed system is consistent with the thermodynamics represented in ISORROPIA, RN/2S and NH_x Fp should not be drastically different in aerosol-only and gas + aerosol mode calculations (see additional lines in Figure 2 and caption). The fact that the predicted RN/2S is very different, indicates that the gas + aerosol input system is inconsistent with the model-predicted ammonia partitioning when only aerosol composition is provided as input. We indicate that one simulation is forced to reproduce RN/2S:

ISORROPIA predictions using AMS measured ammonium and sulfate as input (c), thus exactly reproducing observed $R\{N/2S\}$, showed much higher partitioning of ammonia to the particle phase...

Page 8, lines 12-14: Visually it doesn't look like NH_x Fp for the two CMAQ particles sizes looks very different. Stating values in the text could help make that point clearer.

The values are not meaningfully different.

Page 8, lines 15-17: If ISORROPIA was not sensitive between two different particle sizes, why was CMAQ?

CMAQ uses a modal size distribution. To determine PM₁ and PM_{2.5} the amount of mass below 1 and 2.5 microns respectively is obtained from the Aitken+Accumulation modes. Thus the absolute abundance of ammonium and sulfate is slightly different for PM₁ compared to PM_{2.5}, but the ratio of ammonium to sulfate is not different.

Page 8, lines 20-21: Could a full CMAQ model run with only NH₄, SO₄, NO₃, Cl included in the thermodynamic calculations be done?

The simulation was performed (see response to Reviewer 1). Removing K, Mg, Ca, and Na resulted in CMAQ predicted RN/2S values of 0.96 averaged across the southeastern US CSN sites.

Figure 2: This figure is slightly difficult to interpret given the large amount of information concentrated in it. What significance does the different gray shading have for the box plots – that should be defined in the figure caption. NH_x could be shown on a separate panel to separate some of the information.

The figure was created to compactly show several pieces of information in a limited amount of space. Horizontal lines have been added to help guide the eye. Shading is to visually group different simulations (CMAQ vs ISORROPIA vs AIOMFAC vs observations). Lines have been added to guide the eye and caption updated:

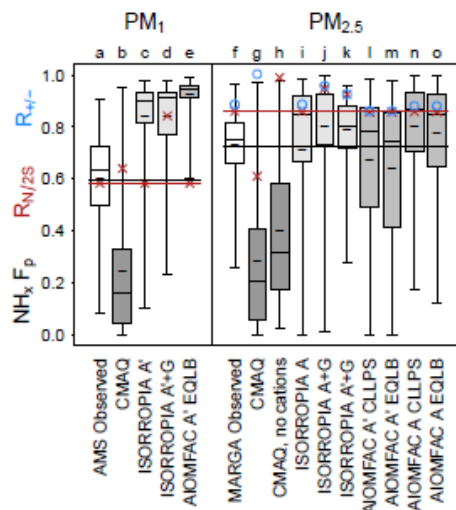


Figure 2. Gas-particle partitioning of ammonia ($\text{NH}_x F_p = \text{ammonium}/(\text{ammonia}+\text{ammonium})$), mean $R_{N/25}$ (red \times), and mean R_{A++} (blue \circ) for $\text{PM}_{1.0}$ measured by the Georgia Tech AMS (Xu et al., 2015a) and $\text{PM}_{2.5}$ measured by a MARGA (Allen et al., 2015) as well as predicted by a CMAQ regional chemical transport model calculation and box models for SOAS conditions at CTR. F_p boxplots indicate the maximum, 75th percentile, median, 25th percentile, and minimum. Short dashes within the boxplots indicate the mean F_p . Box model inputs were either the aerosol (A) or aerosol and gas concentrations (A+G). Box models were run with either the ammonium-sulfate system (A') or including all cations and anions (A). AIOMFAC calculations assumed complete liquid-liquid phase separation between the organic-rich and electrolyte-rich phases (CLLPS) or employed a full equilibrium calculation with organic compounds in which phase separation was calculated based on composition (EQLB). Observed gas-phase ammonia concentrations are from the SEARCH network at CTR. Boxplots are labeled by a letter for easier reference in the text. Shading of the boxplot interquartile range distinguishes different models (CMAQ, ISORROPIA, and AIOMFAC). The horizontal lines correspond to mean observed $\text{NH}_x F_p$ (black) and $R_{N/25}$ (red). A simulation is consistent with observations if it reproduces both $\text{NH}_x F_p$ and $R_{N/25}$.

Page 8, lines 31-32: If organosulfates were not present in large enough concentrations to explain a 20% bias, are there any other explanations? Also, should cite other organosulfate measurements from SOAS (Budisulistiorini et al., 2015; Hettiyadura et al., 2017).

Citations were added. The presence of organosulfates is one hypothesis. If there is an error in how the collection efficiency and adjustment of AMS data is performed, that could be another error. The AMS has a collection efficiency of approximately 50% and thus AMS derived data is corrected to compensate for that.

Furthermore, organosulfates (Budisulistiorini et al., 2015; Hettiyadura et al., 2017) can be measured in the AMS as sulfate. However, organosulfates have been estimated to account for only 5% of AMS-measured sulfate during SOAS (Hu et al., 2017).

Page 9, lines 17-20: What is the reason for the differences between this work and Pye et al. (2017), and which work compares better to observations in terms of expected frequency of phase separation?

The two approaches use different methods. The 2017 paper used an empirical representation of separation relative humidities based on O:C (or OM/OC) without knowledge of the specific organic

aerosol chemical constituents. Observations of phase separation are not available for model comparison. We added “*empirical*” to the description of the previous modeling.

Section 3.4: In discussion of aerosol pH, are there notable differences in aerosol liquid water content between models that would further impact the pH calculations?

This is possible, but we find that AIOMFAC reproduces the ISORROPIA mean pH of 0.7 if operated in the same manner (ie CLLPS mode, assumption of activity coefficient for H+ of 1).

Page 12, lines 9-11: The discussion of improvements required for CMAQ is not sufficient, especially because those errors prevented the use of the full CMAQ results in this study. If the current CMAQ thermodynamic partitioning is not usable, it is important to note if so and why.

We have revised the conclusions (see earlier responses) to highlight that we do not find motivation to change the thermodynamic basis of CMAQ, but need to resolve nonvolatile cation abundance.

Technical corrections

Eastern should not be capitalized on page 2 line 28 for consistency with the rest of the text and US should be U.S. on page 8 line 6.

Corrected

Works Cited

Budisulistiorini, S. H., et al. (2015), Examining the effects of anthropogenic emissions on isoprene-derived secondary organic aerosol formation during the 2013 Southern Oxidant and Aerosol Study (SOAS) at the Look Rock, Tennessee ground site, Atmos. Chem. Phys., 15, 8871-8888, <https://doi.org/10.5194/acp-15-8871-2015>.

Hettiyadura, A. P. S., et al. (2017), Qualitative and quantitative analysis of atmospheric organosulfates in Centreville, Alabama, Atmos. Chem. Phys., 17, 1343-1359, <https://doi.org/10.5194/acp-17-1343-2017>.

Hu, W. W., et al. (2015), Characterization of a real-time tracer for isoprene epoxydiols derived secondary organic aerosol (IEPOX-SOA) from aerosol mass spectrometer measurements, Atmos. Chem. Phys., 15, 11807-11833, <https://doi.org/10.5194/acp-15-11807-2015>.

Other changes:

The order of paragraphs 2 and 3 from section 3.1 were switched to introduce the SEARCH data earlier and hint at inconsistencies in measurements earlier in the manuscript.

The discussion regarding AMS data in section 3.2 was consolidated into the last two paragraphs of the section instead of being located throughout the section. As a result, sentences were reworded. We also wanted to cite the recently published paper by Guo et al. 2017 and a comment on his paper that indicates there may be differences in PM1 vs PM2.5. Consistent with our original manuscript, we still maintain that size alone cannot explain the AMS vs MARGA differences. We also mention the Guo et al.

2017 hypothesis regarding the role of nonvolatile cations, but point out MARGA simulations included those effects.

The inconsistency in AMS data and box models indicated in Figure 2, but ability of models to simulate MARGA data, indicates the AMS data alone may not be suitable for equilibrium thermodynamic modeling. Contributing factors could include: missing ammonium residing in particles larger than PM1 but smaller than PM2.5, potential missing nonvolatile cations, uncertainty in AMS-measured concentrations of sulfate and ammonium, organosulfate contributions to sulfate, or other issues. Guo (2017) indicates differences in ammonium to sulfate ratios for PM1 measured during the first half of SOAS versus PM2.5 measured during the second half of SOAS using the same instrument (the Particle into Liquid Sampler, PILS, (Guo et al., 2017b)) suggesting the role of particle size on ammonium to sulfate ratios. Furthermore, thermodynamic predictions of ammonia were degraded in the work of Guo et al. (2015) when the PILS inlet switched from PM2.5 to PM1. Size alone does not explain the difference in AMS (PM1) vs PM2.5 data as AMS sulfate can be similar to (MARGA) or exceed by 20% (PILS, Guo et al. (2015)) collocated PM2.5 sulfate. Future work that characterizes ammonium and sulfate in PM2.5-PM1 would be helpful for understanding differences in AMS versus other datasets as well as to facilitate connections between AMS data and regulatory metrics including the U.S. NAAQS for PM2.5. Guo et al. (2017b) suggest when AMS (or PILS) data are used together with nonvolatile cations, thermodynamic models can predict ammonia partitioning accurately. However, the levels of nonvolatile cations would need to be larger than current measurements indicate (Guo et al., 2017b). Furthermore, MARGA simulations in this work (Figure 2 j,k) indicated little sensitivity of RN/2S or NHx Fp to inclusion of measured calcium, potassium, magnesium, sodium, nitrate, and chloride.

The differences in the AMS and MARGA datasets in terms of RN/2S are larger than can be explained by known measurement precision. However, uncertainty for AMS measured ammonium (34%) and sulfate (36%) are large (Bahreini et al., 2009). A contributor to this uncertainty is the AMS collection efficiency (CE), and AMS instruments are known to have a higher collection efficiency for acidic (H2SO4-enriched) vs (NH4)2SO4-enriched aerosol (Middlebrook et al., 2012).

A few unnecessary sentences that distracted from the message of the paper were removed. From conclusions.

Removed since we didn't examine diffusivity limitations ourselves:

~~and AIOMFAC thermodynamic calculations, as indicated found in previous model evaluation (Silvern et al., 2017). This behavior could have resulted from a deviation from gas-particle equilibrium, missing thermodynamic effects, or biases in the AMS data. Given that relative humidities are high in the eastern US during summer such that particles should not have diffusivity limitations on a one-hour timescale (Renbaum-Wolff et al., 2013), this work examines the latter two possibilities with an emphasis on the potential bias in AMS data.~~

Removed (unnecessary):

~~allow a large excess of gas-phase ammonia under highly acidic conditions. To improve CMAQ predictions of ammonium to sulfate ratios and, therefore, pH needed for other aerosol processes such as isoprene epoxydiol uptake (Pye et al., 2013), model predictions of nonvolatile cations should be improved in conjunction with ammonia emissions. While consideration~~

Coupling of organic and inorganic aerosol systems and the effect on gas-particle partitioning in the southeastern United States

Havala O. T. Pye¹, Andreas Zuend², Juliane L. Fry³, Gabriel Isaacman-VanWertz^{4,5}, Shannon L. Capps⁶, K. Wyatt Appel¹, Hosein Foroutan¹, Lu Xu⁷, Nga L. Ng^{8,9}, and Allen H. Goldstein^{5,10}

¹National Exposure Research Laboratory, U.S. Environmental Protection Agency, Research Triangle Park, North Carolina, USA

²Department of Atmospheric and Oceanic Sciences, McGill University, Montreal, Québec, CAN

³Department of Chemistry, Reed College, Portland, Oregon, USA

⁴Department of Civil and Environmental Engineering, Virginia Polytechnic Institute and State University, Blacksburg, Virginia, USA

⁵Department of Environmental Science, Policy, and Management, University of California, Berkeley, California, USA

⁶Civil, Architectural, and Environmental Engineering, Drexel University, Philadelphia, Pennsylvania, USA

⁷Department of Environmental Science and Engineering, California Institute of Technology, Pasadena, California, USA

⁸School of Chemical and Biomolecular Engineering, Georgia Institute of Technology, Atlanta, GA, USA

⁹School of Earth and Atmospheric Sciences, Georgia Institute of Technology, Atlanta, Georgia, USA

¹⁰Department of Civil and Environmental Engineering, University of California, Berkeley, California, USA

Correspondence to: Havala O. T. Pye (pye.havala@epa.gov)

Abstract. Several models were used to describe the partitioning of ammonia, water, and organic compounds between the gas and particle phase for conditions in the southeastern United States during summer 2013. Existing equilibrium models and frameworks were found to be sufficient although additional improvements in terms of estimating pure-species vapor pressures are needed. Thermodynamic model predictions were consistent, to first order, with a molar ratio of ammonium to sulfate of approximately 1.6 to 1.8 (Ratio of ammonium to $2 \times$ sulfate, $R_{N/2S} \approx 0.8$ to 0.9) with approximately 70% of total ammonia and ammonium (NH_x) in the particle. Southeastern Aerosol Research and Characterization (SEARCH) network gas and aerosol and Southern Oxidant and Aerosol Study (SOAS) Monitor for Aerosols and Gases in Air (MARGA) aerosol measurements were consistent with these conditions. CMAQv5.2 regional chemical transport model predictions did not reflect these conditions due to biases in a factor of three overestimate of the nonvolatile cations ~~that resulted from either overestimated emissions and/or underestimated mixing~~. In addition, gas-phase ammonia was overestimated in the CMAQ model leading to an even lower fraction of total ammonia in the particle. Chemical Speciation Network (CSN) and Aerosol Mass Spectrometer (AMS) measurements indicated less ammonium per sulfate than SEARCH and MARGA measurements and were inconsistent with thermodynamic model predictions. Organic compounds were predicted to be present to some extent in the same phase as inorganic constituents, modifying their activity and resulting in a decrease in $[\text{H}^+]_{\text{air}}$ (H^+ in $\mu\text{g m}^{-3}$ air), increase in ammonia partitioning to the gas phase, and increase in pH compared to complete organic vs. inorganic liquid-liquid phase separation. In addition, accounting for non-ideal mixing modified the pH such that a fully interactive inorganic-organic system had a pH roughly 0.7 units higher than predicted by traditional methods (pH= 1.5 vs 0.7). Particle-phase interactions of organic and inorganic compounds were found to increase partitioning towards the particle phase (vs. gas phase) for highly oxygenated

(O:C \geq 0.6) compounds including several isoprene-derived tracers as well as levoglucosan, but decrease particle-phase partitioning for low O:C, monoterpene-derived species.

1 Introduction

Ambient particles consist of organic and inorganic compounds. The organic compounds present in the gas and particle phase are diverse and numerous (Goldstein and Galbally, 2007), ranging from relatively unoxidized, long-chain alkanes in fresh emissions to small, highly soluble compounds formed through multiple generations of atmospheric chemistry. Major inorganic constituents include water, sulfate, ammonium, and nitrate with additional contributions from species such as calcium, potassium, magnesium, sodium, and chloride (Reff et al., 2009). The extent to which organic and inorganic components of particulate matter interact within a particle depends on the mixing state (e.g. internal vs external) of the aerosol population as well as degree of phase separation (or number of phases) within the particle. Internally mixed populations, as typically assumed in chemical transport models such as the Community Multiscale Air Quality (CMAQ) model, may exhibit one fairly homogeneous liquid phase state or be heterogeneous in composition. Heterogeneous configurations occur as a result of phase separation and may include a liquid and solid phase or multiple liquid phases. A common heterogeneous configuration under conditions of liquid-liquid or solid-liquid phase separation is that of a core-shell morphology; alternatively, partially engulfed morphologies have been predicted by theory and observed in laboratory experiments (Kwamena et al., 2010; Song et al., 2013; Reid et al., 2011).

Currently, the CMAQ model, as well as other chemical transport models, considers accumulation mode aerosol to form a heterogeneous internal mixture in which organic and inorganic constituents partition between the gas and aerosol phase independently of each other. Pye et al. (2017) examined how assumptions about phase separation of internally mixed particles affect organic aerosol concentrations in the southeast United States as predicted by the CMAQ model. When organic compounds were allowed to mix with the aqueous inorganic phase under conditions of high relative humidity and high degree of oxygenation (You et al., 2013; Bertram et al., 2011; Song et al., 2012), the concentration of organic aerosol was predicted to increase significantly (Pye et al., 2017). While the effects of phase separation on organic compounds are potentially large, they are highly dependent on an accurate parameterization of activity coefficients and a reliable prediction of the composition of individual particle phases (Zuend and Seinfeld, 2012).

Recent work highlights potential discrepancies between current gas-particle partitioning models, which assume equilibrium is attained on short timescales, and observations for both inorganic and organic compounds. Silvern et al. (2017) found that models predict higher ratios of particulate ammonium to sulfate than observed in the ~~Eastern~~eastern U.S. and proposed that organic compounds in an organic-rich phase at the particle surface may reduce ammonia partitioning to the particle via a kinetic inhibition. In addition, organic compound vapor pressure estimation method predictions can vary by orders of magnitude (Topping et al., 2016; O'Meara et al., 2014; Pankow and Asher, 2008) and have often been adjusted downward to improve model predictions (Chan et al., 2009; Johnson et al., 2006). Furthermore, isoprene-epoxydiol-derived organic aerosol partitions to the particle phase to a greater degree than structure-based vapor pressures would suggest (Isaacman-VanWertz et al., 2016;

Lopez-Hilfiker et al., 2016; Hu et al., 2016). Since $PM_{2.5}$ (particulate matter concentration from particles of diameters less than $2.5 \mu m$) is regulated via the National Ambient Air Quality Standards (NAAQS) in the U.S., while similar ambient standards are not set for the gas-phase counterparts (NH_3 [and organic compound vapors](#)), errors in partitioning will affect model performance with implications for metrics used in regulatory applications. The model sensitivity of $PM_{2.5}$ to emission changes can also be too high or too low if compounds are erroneously partitioned.

In this work, gas-particle partitioning of ammonia and several isoprene-, monoterpene-, and biomass burning-derived organic compounds was examined using common air quality modeling treatments and advanced approaches. Results address the degree to which techniques accounting for organic-inorganic interactions, deviations in ideality, and phase separation reproduce observations. Models were evaluated for their ability to predict ammonia versus ammonium as well as gas-particle partitioning of organic compounds. In addition, the effects of organic compounds on aerosol pH were examined.

2 Methods

2.1 Model Approaches

Several box-model approaches as well as CMAQ regional chemical transport model calculations were used to represent the partitioning of compounds between the gas and particle phases. CMAQ version 5.2-gamma was run over the continental U.S. at 12 km by 12 km horizontal resolution for 1 June – 15 July 2013, coinciding with the Southern Oxidant and Aerosol Study (SOAS) field campaign and the Centreville, Alabama, U.S. field site. WRF v3.8 meteorology with lightning assimilated into the convection scheme (Heath et al., 2016) was processed for use with the CMAQ model (Otte and Pleim, 2010). Emissions were based on the 2011 National Emission Inventory version 2 ~~and~~ [\(ek\). Emissions influenced by model meteorology \(biogenic compounds, mobile sector\) or monitored \(electrical generation units\) were](#) year 2013 specific ~~when available~~. Windblown dust emissions followed the scheme of Foroutan et al. (2017). Ammonia emissions and deposition from croplands were parameterized as a bidirectional exchange (Pleim et al., 2013). CMAQ used ISORROPIA v2.1 (Fountoukis and Nenes, 2007; Nenes et al., 1998) with gas and aerosol composition and environmental conditions (temperature, relative humidity) as input to predict the Aitken and Accumulation mode ammonium, nitrate, and chloride mass concentrations. CMAQ predicted PM_1 and $PM_{2.5}$ were computed based on the fraction of the Aitken and Accumulation modes less than 1 or 2.5 microns in diameter as appropriate (Nolte et al., 2015).

Consistent with the CMAQ regional model, partitioning of ammonia between the gas and particle phases was also predicted using ISORROPIA as a box model driven with observed aerosol [\(reverse mode\)](#) or gas and aerosol [\(forward mode\)](#) concentrations of ammonia, ammonium, nitrate, nitric acid, calcium, potassium, magnesium, sodium, and chloride. Output from the ISORROPIA box-model was either gas-phase ammonia in equilibrium with the observed aerosol ammonium [\(reverse mode\)](#), or ammonia vs. ammonium based on total gas and aerosol conditions [\(forward mode\)](#). ISORROPIA does not consider the effects of organic compounds on aerosol pH or explicitly treat liquid-liquid phase separation.

Algorithms that allowed for inorganic-organic interactions were applied using a thermodynamic equilibrium gas-particle partitioning model (Zuend et al., 2010; Zuend and Seinfeld, 2012) based on the Aerosol Inorganic-Organic Mixtures Func-

tional groups Activity Coefficients (AIOMFAC) model (Zuend et al., 2008, 2011). AIOMFAC provided an estimate of activity coefficients for aerosol systems of specified functional group composition, which was used in two modes: (i) predefined complete liquid-liquid phase separation (CLLPS) in which the organic compounds did not mix with the inorganic salts and (ii) equilibrium (EQLB) in which the Gibbs energy of the system was minimized and up to two liquid phases of any composition were allowed to form in the particle as predicted by a modified liquid-liquid phase separation algorithm based on the method by Zuend and Seinfeld (2013). For purposes of AIOMFAC calculations, observed calcium, potassium, and magnesium concentrations were converted to charge-equivalent sodium amounts since the former's interactions with the bisulfate ion in solution are not treated by the model.

Several quantities, including pH and molar ratios, were calculated to evaluate the inorganic aerosol system. Solution acidity can be expressed in different ways, the most common one being the pH value. However, many definitions of pH exist, with several definitions only applicable to highly dilute aqueous solutions. Thermodynamics-based pH definitions vary with the choice of composition scale (molality, molarity, or mole fraction basis) and the solvent into which H^+ is assumed to dissolve, which may be strictly water associated with inorganic constituents as in ISORROPIA II, or include the diluting effect of water associated with organic compounds (Guo et al., 2015), organic compounds themselves (Zuend et al., 2008), or other aerosol constituents (Budisulistiorini et al., 2017). Furthermore activity coefficients of H^+ may not be unity as is frequently assumed. In this work, pH was defined following the thermodynamic definition on a molality basis, as recommended by IUPAC (<http://goldbook.iupac.org/html/P/P04524.html>) and computed by the AIOMFAC model. By expressing the molality of H^+ in terms of concentration per volume of air, the following results:

$$pH = -\log_{10}(\gamma_{H^+}[H^+]_{\text{air}}/[S]) \quad (1)$$

where γ_{H^+} is the molality based activity coefficient for H^+ in the liquid phase, $[H^+]_{\text{air}}$ is the concentration of the hydronium ion in the liquid phase in moles per volume of air and $[S]$ is the solvent mass in that liquid phase (kg per volume of air), i.e. $[H^+]_{\text{air}}/[S]$ is the molality of H^+ . The solvent included water associated with inorganic compounds (W_i), water associated with organic compounds (W_o), and organic compounds (C_{org}) as appropriate based on the predicted phase composition. ISORROPIA pH calculations assumed $[S] = [W_i]$ and an activity coefficient of unity thus following previous methods (Guo et al., 2017a). The molar ratio of ammonium to 2 × sulfate was defined as:

$$R_{N/2S} = \frac{n_{\text{NH}_4^+}}{2 \times n_{\text{SO}_4^{2-}}}, \quad (2)$$

and the electric charge normalized molar ratio of cations to anions that participate in ISORROPIA was:

$$R_{+/-} = \frac{n_{\text{NH}_4^+} + n_{\text{Na}^+} + 2 \times n_{\text{Ca}^{2+}} + n_{\text{K}^+} + 2 \times n_{\text{Mg}^{2+}}}{2 \times n_{\text{SO}_4^{2-}} + n_{\text{NO}_3^-} + n_{\text{Cl}^-}}. \quad (3)$$

Since ambient measurements and CMAQ model output do not distinguish bisulfate from sulfate, the sulfate in these ratios represented total sulfate ($\text{SO}_4^{2-} + \text{HSO}_4^-$).

To employ the AIOMFAC-based equilibrium models, organic aerosol positive matrix factorization (PMF) analysis results of ambient data (next section) were converted to molecular structures of known functional group composition as surrogates for a

range of organic compound classes in ambient particles as described in Tables S1-S3 thus providing a complete characterization of the organic aerosol partitioning medium. Several isoprene-derived (2-methyltetrols, C₅-alkene triols, 2-methylglyceric acid) and monoterpene-derived (pinic acid, pinonic acid, hydroxyglutaric acid) compounds as well as levoglucosan, a semivolatile indicator of biomass burning, were explicitly represented in box-model calculations. Pure species' vapor pressures (sub-cooled liquid) were obtained via the EVAPORATION model (Compernelle et al., 2011). The temperature dependence was parameterized by using the same Antoine-like function that is also employed by the EVAPORATION model. A sensitivity calculation (referred to as Adj Psat) reduced EVAPORATION-based vapor pressures by a factor of 4.2, thus maintaining the compound to compound variability predicted by EVAPORATION but correcting for potential overestimates in pure compound vapor pressures. The magnitude of the adjustment was based on the effective saturation concentration obtained via regression needed to reproduce observations in a traditional absorptive partitioning framework (Equation S1). This adjustment factor is similar in magnitude to the difference between SIMPOL (Pankow and Asher, 2008) and EVAPORATION (Compernelle et al., 2011) predicted vapor pressures for several species, but not all (see Table S4). The effective saturation concentration, C*, of a species, i, was defined as (Zuend and Seinfeld, 2012):

$$C_i^* = \frac{C_i^g \sum C_k^{PM}}{C_i^{PM}} \quad (4)$$

where C_i^g is the mass-based gas-phase concentration of species i , C_i^{PM} is the mass-based liquid-phase concentration of species i , and C_k^{PM} is the total mass-based concentration of the liquid phase where the summation index k includes organic species, inorganic species, and water. See Equation S2 for C_i^* in terms of the mole-fraction based activity coefficient.

2.2 Ambient Data

Regional model predictions of inorganic aerosol were evaluated against the Chemical Speciation Network (CSN) and Southeastern Aerosol Research and Characterization (SEARCH) network observations (at different ground sites). [The Interagency Monitoring of Protected Visual Environments \(IMPROVE\) network \(Solomon et al., 2014\) also measures some chemical speciation of PM_{2.5} throughout the U.S., but does not include ammonium.](#) CSN determines anions and cations via ion chromatography of extracts from nylon filters (Solomon et al., 2014). [Solomon et al. \(2014\) estimate the precision of CSN measured ammonium is 11% and sulfate is 7% \(for co-located samples during 2012\) but the actual measurement uncertainty is likely higher \(and not quantified\).](#) The SEARCH network [operates at fewer sites and exclusively in the Southeast U.S. It](#) uses a multichannel approach employing nylon, teflon, and citric acid-coated cellulose filters to measure speciated 24-hour average PM_{2.5} (Edgerton et al., 2005). [SEARCH reports the precision of measured sulfate and ammonium in PM_{2.5} is 2-3% \(Egerton et al., 2005\).](#) The SEARCH 24-hour filter measurements are also used to adjust the co-located continuous measurements (Edgerton et al., 2006).

In addition to the network data, ambient data from SOAS at the Centreville, AL (CTR; 87.25° W, 32.90° N) site from June and July, 2013 were used as input to the box models and for model evaluation. The High Resolution Time of Flight Aerosol Mass Spectrometer (HR-ToF-AMS, hereafter AMS) operated by the Georgia Institute of Technology was the primary source of SOAS PM₁ organic mass, ammonium, and sulfate (Xu et al., 2015a). [This AMS dataset was consistent with the other AMS instrument operating at CTR as well as AMS measurements aboard an aircraft over the southeastern U.S. \(Table](#)

S5-S6). When AMS data was used as input in PM₁ box modeling, inorganic nitrate was set to zero as nitrate measured by the AMS contained significant contributions from organic nitrogen-containing compounds (Xu et al., 2015b). Thus, AMS calculations assumed the inorganic aerosol was composed only of ammonium, sulfate, bisulfate, and the hydronium ion (referred to in subsequent sections as the A' system). The assignment of measured ammonium and sulfate to specific salts (ammonium sulfate vs ammonium bisulfate) for use as input electrolyte components to AIOMFAC was determined by mass balance. ~~For ammonium-sulfate only conditions in which the moles $\geq 2\times$, a small amount ($1 \times 10^{-4} \mu\text{g}$) of ammonium bisulfate was added to the AIOMFAC input in order to trigger a potential partial association of sulfate and ions to bisulfate following the equilibrium constant of that reaction.~~ Inorganic PM_{2.5}, including ammonium, sulfate, nitrate, calcium, potassium, magnesium, sodium, and chloride, was measured at CTR by a Monitor for Aerosols and Gases in Air (MARGA) (Allen et al., 2015). Less than 5% of the PM_{2.5} MARGA data used in this work had elevated nitrate ($>0.8 \mu\text{g m}^{-3}$) due to supermicron crustal material and sea salt episodes (Allen et al., 2015). ~~Gas-phase~~ The data from MARGA was used in two ways for model calculations with AIOMFAC. (1) All the measured ion concentrations were considered, but the molar amounts of the cations Ca^{2+} , K^{+} , Mg^{2+} , and Na^{+} were mapped to a charge-equivalent amount of Na^{+} (see Section 2.1). (2) Only the measured concentrations of ammonium and sulfate ions were considered and mapped to the electrolyte components ammonium sulfate, ammonium bisulfate, and sulfuric acid for AIOMFAC model input purposes. For ammonium-sulfate only conditions (option 2) in which the moles $\text{NH}_4^{+} \geq 2 \times \text{SO}_4^{2-}$, a small amount ($1 \times 10^{-4} \mu\text{g m}^{-3}$) of ammonium bisulfate was added to the AIOMFAC input for MARGA calculations in order to trigger a potential partial association of sulfate and H^{+} ions to bisulfate following the equilibrium constant of that reaction. Such conditions did not occur with AMS data. Hourly gas-phase ammonia was obtained from the CTR SEARCH network site via a corrected Thermo Scientific citric acid-impregnated denuder. Relative humidity (RH) and temperature were obtained from the routine SEARCH network measurements at the SOAS site.

The entire organic aerosol composition was characterized in terms of functional groups for use with AIOMFAC. The semi-volatile thermal desorption aerosol gas chromatograph (SV-TAG) with in situ derivatization (Isaacman-VanWertz et al., 2016; Isaacman et al., 2014) provided measured gas- and aerosol-phase concentrations of 2-methyltetrols, C₅-alkene triols, 2-methylglyceric acid, pinic acid, pinonic acid, hydroxyglutaric acid, and levoglucosan. More oxidized-oxygenated organic aerosol (MO-OOA), biomass burning organic aerosol (BBOA), Isoprene-OA, and less oxidized-oxygenated organic aerosol (LO-OOA) PMF factors from the AMS were represented with specific functional groups and associated surrogate chemical structures (Table S1). As previous work indicates a fraction of measured 2-methyltetrols may be decomposition products of low-volatility accretion products (Isaacman-VanWertz et al., 2016; Lopez-Hilfiker et al., 2016), 50% (as a rough estimate) of measured 2-methyltetrols (in the particle phases) were assumed to be dimer decomposition products when EVAPORATION-based vapor pressures were used (see Table S4). In the sensitivity calculation (Adj Psat), 2-methyltetrols were assumed to be present only in the monomer form as including dimers increased the model bias.

The overlap in the input data sets resulted in 180 hours of measurement coverage. Additional measurements of ammonium, sulfate, and ammonia (not used in this work) are summarized in Tables S5-S7 for reference.

3 Results and Discussion

3.1 Regional ammonium-sulfate conditions

Figure 1 shows the molar ratios of ammonium to $2 \times$ total sulfate and cations to anions over the eastern U.S. for 1 June - 15 July 2013 based on observations from the CSN network and predicted by CMAQv5.2. CMAQ predicted a mean $R_{N/2S}$ of 0.73 over the U.S. compared to the observed mean of 0.67. The model showed higher values (near 1) over the central U.S. and lower values (<0.6) over the southeast U.S. The magnitude of the ~~observed $R_{N/2S}$ was similar to CMAQ predicted $R_{N/2S}$ over the southeast U.S. (mean of 0.6) was only slightly higher than~~ that from the CSN network (mean of 0.4). ~~CMAQ-predicted sulfate was relatively unbiased in the southeastern U.S. (normalized mean bias $<10\%$). However of 5% compared to CSN), but ammonium was high by a factor of 1.5 (Table S10). Despite only a moderate bias in $R_{N/2S}$,~~ significant discrepancies existed between the model and observations for the ratio of cations to anions. ~~The observations indicated that the ratio of ammonium to sulfate was a good proxy for the ratio of cations to anions.~~ In CMAQ, however, the ratio of cations to anions was approximately one ~~indicating that ammonia tended to be pulled into the particle in an amount necessary to neutralize sulfate not already associated with nonvolatile cations.~~ Molar ratios are not robust indicators of aerosol pH (Hennigan et al., 2015) as a result of the role of relative humidity and associated liquid water content as well as buffering by bisulfate (Guo et al., 2015). However, chemical transport model biases in ion ratios should result in biases in acidity and gas-particle partitioning of volatile acids and bases (e.g. NH_3) considering other factors (such as RH) held constant.

~~An evaluation of the individual cations and anions (Figures S1-S5) indicates CMAQ over-predicted the non-volatile ISORROPIA cations (Na^+ , Ca^{2+} , K^+ , Mg^{2+}) which was not revealed in the $R_{N/2S}$ comparison in Figure 1. Appel et al. (2013) have previously shown that even when anthropogenic fugitive dust and windblown dust emissions are removed from the CMAQ model, crustal elements are still typically overestimated compared to observations. Coal combustion, for example, is a major source of trace metals in the U.S. (Reff et al., 2009). Trace metal emissions were overestimated (and/or physical mixing was underestimated) since CMAQ overestimated their measured concentration, which included soluble and insoluble contributions (Solomon et al., 2014). Since ISORROPIA should only consider the cations associated with sulfate, nitrate, and chloride, but CMAQ includes cations that are part of insoluble metal oxides (Reff et al., 2009), additional error was incurred in CMAQ by allowing all of the calcium, potassium, magnesium, and sodium present in aerosol to participate in ISORROPIA calculations. Thus, the apparent consistency in ammonium to sulfate ratios between CSN and CMAQ, should not be used to confirm the reasonableness of either. The ratio of cations to anions indicates discrepancies between CSN and CMAQ, specifically, that the CMAQ model tends to achieve charge balance as defined by $R_{T-}=1$ while observations indicate otherwise.~~

Also included in Figure 1(a-b) are observations of $R_{N/2S}$ based on the SEARCH network (triangles) which are much higher (>0.8) than the CSN values (<0.6) in the southeast U.S. While there could be spatial heterogeneity in the southeast U.S., differences so large are unlikely and not present in CMAQ, thus indicating potential problems in one set of measurements. Nylon filters (used by CSN for inorganic ions) can collect 4-5% of gas-phase sulfur dioxide (Benner et al., 1991; Hansen et al., 1986), leading to a small but positive sulfate mass concentration artifact. In addition, nylon filters tend to measure lower ammonium concentrations than other filter types (Solomon et al., 2000; Yu et al., 2006). These ammonium artifacts are not

restricted to ammonium nitrate since more than twice as much NH_4^+ was lost compared to nitrate on nylon filters from Great Smoky Mountains National Park, TN, U.S. (Yu et al., 2006). 6-14% of total NH_4^+ can volatilize in federal reference method (FRM) collection, and the SEARCH network best estimates of $\text{PM}_{2.5}$ result in higher ammonium on an absolute basis and as a fractional contribution to $\text{PM}_{2.5}$ compared to the FRM equivalent mass (Edgerton et al., 2005). Consider that a 10% underestimate in ammonium PM and 10% overestimate in sulfate, for example, will lead to almost a 20% underestimate in $R_{\text{N}/2\text{S}}$.

An overabundance of cations in the CMAQ model (Figure S1, Table S10) means that ammonium was displaced from the particle and $R_{\text{N}/2\text{S}}$ was biased low for the southeast U.S. An evaluation of the individual cations and anions (Figure S1, Table S10) indicated CMAQ over predicted the non-volatile ISORROPIA cations (Na^+ , Ca^{2+} , K^+ , Mg^{2+}) by factors of 2 to 6 individually and by a charge equivalent factor of 3 overall in the Southeast. A factor of 3 overestimate in nonvolatile cations indicates ammonium predicted by CMAQ was low by about 26%. Appel et al. (2013) have previously shown that even when anthropogenic fugitive dust and windblown dust emissions are removed from the CMAQ model, crustal elements are still typically overestimated compared to observations. Coal combustion, for example, is a major source of trace metals in the U.S. (Reff et al., 2009). Trace metal emissions were overestimated (and/or physical mixing was underestimated) since CMAQ overestimated their measured concentration, which included soluble and insoluble contributions (Solomon et al., 2014). A sensitivity simulation in which all Aitken and accumulation mode Na^+ , Ca^{2+} , K^+ , and Mg^{2+} were removed from the partitioning thermodynamics resulted in a mean predicted $R_{\text{N}/2\text{S}}$ of 0.96 for the southeast U.S. Since ISORROPIA should only consider the cations associated with sulfate, nitrate, and chloride, but CMAQ includes cations that are part of insoluble metal oxides (Reff et al., 2009), additional error was incurred in CMAQ by allowing all of the calcium, potassium, magnesium, and sodium present in aerosol to participate in ISORROPIA calculations. Thus, the apparent consistency in ammonium to sulfate ratios between CSN and CMAQ, should not be used to confirm the reasonableness of either. The ratio of cations to anions indicates discrepancies between CSN and CMAQ, specifically, that the CMAQ model tends to achieve charge balance as defined by $R_{\text{+/-}}=1$ while observations indicate otherwise.

3.2 Ammonia gas-particle partitioning during SOAS

Consistent with CMAQ predictions over the greater southeastern U.S. region, CMAQ predicted an average ratio of ammonium to $2 \times$ sulfate ($R_{\text{N}/2\text{S}}$) of 0.64-0.61 (for PM_1 and $\text{PM}_{2.5}$ respectively) and 24-28% of total ammonia in the particle as ammonium (b and g in Figure 2) at CTR. CMAQ also predicted that the cation to anion charge ratio, $R_{\text{+/-}}$, was near one during SOAS. Thus, CMAQ predictions for SOAS CTR site were representative of the southeastern United States for further investigating CMAQ model issues related to inorganic molar ratios and ammonia partitioning.

As shown in Figure 2, the CMAQ predicted $R_{\text{N}/2\text{S}}$ (b) was similar to the Georgia Tech AMS derived value (a). It was also similar to the regional SEAC⁴RS AMS-derived values (Silvern et al., 2017) (Table S6) which averaged near 0.6. ISORROPIA predictions using AMS measured ammonium and sulfate as input (c), thus exactly reproducing observed $R_{\text{N}/2\text{S}}$, showed much higher partitioning of ammonia to the particle phase (mean $\text{NH}_x F_p$ of 0.8) than indicated by AMS aerosol data combined with SEARCH ammonia. Using total ammonia and ammonium as model input resulted in a similar fraction of NH_x in the

particle as using only ammonium-aerosol composition as input, but the $R_{N/2S}$ value significantly increased to around 0.8 (d). The AIOMFAC-based equilibrium model run with aerosol-only inputs (e) was qualitatively consistent with ISORROPIA (c) in terms of the fraction of NH_x in the particle. ~~These~~ Since no box model simulation of AMS data in this work was able to reproduce both the $NH_x F_p$ and $R_{N/2S}$, these tests indicated that AMS measurements at SOAS CTR were inconsistent with

5 ISORROPIA and AIOMFAC thermodynamic calculations, as indicated-found in previous model evaluation (Silvern et al., 2017). ~~This behavior could have resulted from a deviation from gas-particle equilibrium, missing thermodynamic effects, or biases in the AMS data. Given that relative humidities are high in the eastern US during summer such that particles should not have diffusivity limitations on a one-hour timescale (Renbaum-Wolff et al., 2013), this work examines the latter two possibilities with an emphasis on the potential bias in AMS data.~~

10 The $R_{N/2S}$ determined from the MARGA instrument for $PM_{2.5}$ (f) was significantly higher than that derived from the AMS measurements and closer to the values based on SEARCH measurements (Table S5, Figure 1). The AMS tended to measure much less ammonium ~~and the same or slightly less sulfate~~ than the MARGA ~~thus biasing the AMS-determined $R_{N/2S}$ low (Table S5-S6).~~ As, and as a result, the fraction of ammonia partitioned to the particle using SEARCH NH_3 and MARGA aerosol measurements was higher than would be estimated using AMS data. The CMAQ model calculations showed a small but similar

15 trend as observations for PM_1 to $PM_{2.5}$ in terms of ammonia gas-particle partitioning (since $PM_{2.5} \geq PM_1$ and $F_p = PM / (PM + gas)$) but did not show significantly increased $R_{N/2S}$ with increased particle size. Note that in full CMAQ model calculations, the predicted nonvolatile cation concentrations were so high that they erroneously affected the partitioning of ammonium (Table S10, Figure S1). Removing nonvolatile cations from CMAQ (h) allowed more ammonium into the particle and led to increased $R_{N/2S}$, but $NH_x F_p$ was still low indicating overestimates in gas-phase ammonia in the CMAQ model are

20 not primarily due to the displacement of ammonium by nonvolatile cations.

ISORROPIA $PM_{2.5}$ calculations using both gas and aerosol inputs were run with ~~(i-j~~ in Figure 2) and without ~~(j-k)~~ aerosol calcium, potassium, magnesium, sodium, nitrate, and chloride and the results were qualitatively the same in terms of mean fraction of ammonia partitioned to the particle and ratio of NH_4^+ to sulfate in the particle. Thus, the difference between ~~and~~ AMS and MARGA was primarily driven by the difference in ammonium and sulfate measured by the AMS versus MARGA

25 instrument, not the ~~difference in size of particles sampled or the~~ availability of nonvolatile cations. Comparing the change in mean $NH_x F_p$ with (m) and without (l) organic compound interactions indicates that organic compounds have a larger effect on ammonia gas-particle partitioning than the inclusion (j) or lack (k) of calcium, potassium, magnesium, sodium, nitrate, and chloride. Overall, ISORROPIA and AIOMFAC were qualitatively consistent with MARGA measurements of $R_{N/2S}$, but not with AMS measurements. ~~Note that in full CMAQ model calculations, the nonvolatile cations were so high that they~~

30 ~~erroneously affected the partitioning of ammonium.~~

The inconsistency in AMS data and box models indicated in Figure 2, but ability of models to simulate MARGA data, indicates the AMS data alone may not be suitable for equilibrium thermodynamic modeling. Contributing factors could include: missing ammonium residing in particles larger than PM_1 but smaller than $PM_{2.5}$, potential missing nonvolatile cations, uncertainty in AMS-measured concentrations of sulfate and ammonium, organosulfate contributions to sulfate, or other issues. Guo (2017) indicates differences in ammonium to sulfate ratios for PM_1 measured during the first half of SOAS

versus $PM_{2.5}$ measured during the second half of SOAS using the same instrument (the Particle into Liquid Sampler, PILS, (Guo et al., 2017b)) suggesting the role of particle size on ammonium to sulfate ratios. Furthermore, thermodynamic predictions of ammonia were degraded in the work of Guo et al. (2015) when the PILS inlet switched from $PM_{2.5}$ to PM_{1} . Size alone does not explain the difference in AMS (PM_{1}) vs $PM_{2.5}$ data as AMS sulfate can be similar to (MARGA) or exceed by 20% (PILS, Guo et al. (2015)) collocated $PM_{2.5}$ sulfate. Future work that characterizes ammonium and sulfate in $PM_{2.5}$ - PM_{1} would be helpful for understanding differences in AMS versus other datasets as well as to facilitate connections between AMS data and regulatory metrics including the U.S. NAAQS for $PM_{2.5}$. Guo et al. (2017b) suggest when AMS (or PILS) data are used together with nonvolatile cations, thermodynamic models can predict ammonia partitioning accurately. However, the levels of nonvolatile cations would need to be larger than current measurements indicate (Guo et al., 2017b). Furthermore, MARGA simulations in this work (Figure 2 j,k) indicated little sensitivity of $R_{N/2S}$ or $NH_x F_p$ to inclusion of measured calcium, potassium, magnesium, sodium, nitrate, and chloride.

The differences in the AMS and MARGA datasets in terms of the AMS and MARGA datasets in terms of $R_{N/2S}$ are consistent with a potential bias in AMS collection efficiency (CE) for ammonium sulfate vs ammonium bisulfate and/or the presence of organosulfates in AMS measured sulfate. are larger than can be explained by known measurement precision. However, uncertainty for AMS instruments are known to have a higher collection efficiency for acidic (measured ammonium (34%) and sulfate (36%) are large (Bahreini et al., 2009). A contributor to this uncertainty is the AMS collection efficiency (CE), and AMS instruments are known to have a higher collection efficiency for acidic (H_2SO_4 -enriched) vs (NH_4) $_2$ SO_4 -enriched aerosol and a composition dependent collection efficiency is applied to ambient data (Middlebrook et al., 2012). If there was a bias in the calculated CE as a function of $R_{N/2S}$, it would lead to a bias in measured $R_{N/2S}$. The magnitude of this potential bias is not clear. If the difference in AMS vs MARGA data was a result of measurement of by the AMS vs by MARGA, then AMS measured ammonium and sulfate concentrations should always be lower than measurements, which is not the case. Guo et al. (2015) compared Georgia Tech AMS measurements to the Particle into Liquid Sampler (PILS) measurements and showed that AMS sulfate was high (by 20%) compared to PILS measured sulfate, implying the AMS has a low. A portion of the AMS overestimate in sulfate (relative to ammonium) may be due to organosulfates which accounted for roughly aerosol (Middlebrook et al., 2012). Furthermore organosulfates (Budisulistiorini et al., 2015; Hettiyadura et al., 2017) can be measured in the AMS as sulfate. However, organosulfates have been estimated to account for only 5% of measured AMS-measured sulfate during SOAS (Hu et al., 2017).

3.3 Phase composition

Figure 3 shows the average concentration of aerosol components predicted in the electrolyte-rich (α) and organic-rich (β) aerosol phases as well as under conditions in which only one liquid phase was predicted (single phase) based on AIOMFAC equilibrium calculations (EQLB) of the aqueous ammonium-sodium-sulfate-nitrate-chloride (A) and organic surrogates system. In all cases, water was predicted to be a major contributor to the phase accounting for 60%, 35%, and 90% of the mass in the average α , β , and single phases respectively. In addition, inorganic ions were present in all phases including the organic-rich phase. This means that the effects of inorganic species on organic compounds were not limited to times when one single liquid

phase was predicted. Higher concentrations of organic species were generally associated with an increase in the predicted frequency of phase separation. However, LO-OOA, the least oxygenated (Table S2) and least water-soluble secondary organic aerosol PMF factor (Xu et al., 2017), was not more or less abundant when phase separated vs. single phase conditions were predicted.

The mean $R_{N/2S}$ varied slightly by phase with the α phase having a value of 0.8 and the phases with a greater proportion of organic compounds (β and single) having a value of 0.9. The β phase, with its **high-higher** concentration of organic species, showed a lower average $[H^+]_{air}$ (0.1 nmol m^{-3}) compared to the α phase (1.5 nmol m^{-3}), while the activity-based pH values were predicted to be similar in both phases, typically within 0.2 pH units (as expected from equilibrium thermodynamics). The ammonium-sulfate only (in terms of inorganic ion representation) system was predicted to have the same frequency of phase separation and trend in $[H^+]_{air}$, but less difference in the $R_{N/2S}$ between the phases.

Phase separation into electrolyte-rich and organic-rich phases was predicted to occur 70% of the time. The frequency of phase separation predicted for SOAS conditions was higher than the frequency predicted in previous CMAQ work (Pye et al., 2017) that calculated separation relative humidities based on average O:C ratios using the empirical parameterization of You et al. (2013) for a particular inorganic salt type. Both the previous CMAQ calculations (Pye et al., 2017) and this work predicted the same diurnal variation with a greater frequency of phase separation during the day driven by lower relative humidities (Figure S9S7).

3.4 Effects of organic compounds on acidity

Acidity (pH) is an important aerosol property as it promotes dissolution of metals (Fang et al., 2017), increases nutrient availability (Stockdale et al., 2016), and catalyzes particle-phase reactions (Eddingsaas et al., 2010). Current recommended methods for estimating aerosol pH include thermodynamic models and ammonia-ammonium partitioning (Hennigan et al., 2015) as direct measurements are difficult to make (Rindelaub et al., 2016). AIOMFAC predicted a median molal pH of 1.4 (ammonium-sulfate system) to 1.5 (ammonium-sodium-sulfate-nitrate-chloride system) for SOAS conditions (Table 1). AIOMFAC occasionally showed high pH (pH = 7, Figure 4) which occurred when an excess of cations compared to anions were observed, leading to the absence of H^+ and bisulfate in the input compositions used with the model. Similar behavior has occurred with ISORROPIA and the AIM thermodynamic models using aerosol-only inputs (Hennigan et al., 2015) and likely resulted from measurement uncertainty and a resulting high-bias in the measured amounts of cations compared to charge-equivalent anions. The ISORROPIA predicted pH for the subset of conditions used here (pH = 0.7 to 1.1) was similar to those previously reported for SOAS (pH = 0.9) and Southeast Nexus (SENEX) aircraft campaign (pH = 1.1) using other datasets as summarized by Guo et al. (2017a).

Regardless of whether only ammonium-sulfate or ammonium-sodium-sulfate-nitrate-chloride systems were treated, AIOMFAC predicted an increase in the concentration of gas-phase ammonia (decrease in $NH_x F_p$, Figure 2 m compared to l or o compared to n) along with a decrease in acidity when organic compounds were considered in the calculation of partitioning (EQLB vs CLLPS, Table 1, Figure 4). The presence of organic compounds in the same phase as H^+ and other ions (EQLB case) shifted free H^+ towards increased association with sulfate to form bisulfate as AIOMFAC predicts bisulfate to be more

miscible with organic compounds than H^+ and other small cations. Interactions with organic compounds resulted in a 34-36% decrease in median $[H^+]_{air}$ and a 0.1 unit increase (11-12% increase) in median pH.

5 If the pH for forced complete phase separation conditions was recalculated using AIOMFAC CLLPS predicted $[H^+]_{air}$ and assuming an activity coefficient of one (traditional method), the resulting pH has a median of 0.7 (Figure 4b), the same value obtained by ISORROPIA using only aerosol inputs and an activity coefficient of unity. Thus, traditional methods resulted in an artificially low pH. Taking into account activity coefficients other than unity, phase separation, and the diluting effect of organic compounds and their associated water (EQLB) resulted in a pH 0.7 pH units higher than traditional methods. This increase is substantial given that the pH scale is logarithmic; a 0.7 pH unit higher value is equivalent to a five times lower molal H^+ activity in solution. The activity coefficient value was a major driver of this difference with a secondary role for solvent abundance and change in $[H^+]_{air}$.

3.5 Partitioning of organic compounds under ambient conditions

For organic compounds with $O:C \geq 0.6$ (C_5 -alkene triols, levoglucosan, 2-methyltetrols, hydroxyglutaric acid, 2-methylglyceric acid), the particle-phase fraction, F_p , was predicted to increase when the electrolyte-rich and organic-rich phases were allowed to equilibrate (EQLB compared to CLLPS, Figures 5-6) as a result of an increase in the abundance of the partitioning medium. For compounds with lower O:C (specifically pinic and pinonic acid) F_p decreased as a result of unfavorable liquid-phase interactions. The increase in F_p for most species generally resulted in a decrease in the mean bias and mean error of F_p compared to observations (Figure 5b). With the pure-species adjusted vapor pressure (Adj Psat sensitivity), the mean bias in F_p for all organic species was less than 0.2 and emphasized that information about the pure species vapor pressure is important for accurate gas-particle partitioning calculations. The influence of inorganic constituents on organic compound partitioning was not limited to the times when one single phase was present. In the case of hydroxyglutaric acid (Figure 6g), predictions of F_p were found to be most sensitive to assumptions regarding condensed phase mixing during the day when phase separation was most common (coinciding with a lower average RH during midday and afternoon hours, as expected). This occurred because the organic-rich phase still contained a significant amount of inorganic ions (Figure 3) which modified the partitioning medium and impacted the predicted activity of the organic species.

The change in F_p between CLLPS and EQLB calculations was consistent with the change in effective saturation concentrations (Figure 5c). The effective C^* (equation 4) under equilibrium (EQLB) conditions compared to CLLPS (EQLB $C^*/$ CLLPS C^*) was a strong function of the compound O:C ratio (Pearson's $r^2=0.79$) with higher O:C species having lower EQLB $C^*/$ CLLPS C^* ratios. The mean activity coefficient value was predicted to either stay the same (2-methylglyceric acid) or increase (all other explicit organic species) in EQLB compared to CLLPS. Thus, the driving factor for increased partitioning to the particle phase (indicated by increased F_p and decreased C^*) for species with $O:C > 0.6$ under EQLB compared to CLLPS was the ability of the increased partitioning medium size to overcome the increased activity coefficients. The increased partitioning medium gained by interacting with the inorganic species and their water lowered the mole fraction of the organic species in the particle, thus leading to lower predicted particle-phase activity and gas-phase concentrations via modified Raoult's law. In some cases, like for 2-methyltetrols, the species exhibited negative deviations from ideality ($\gamma < 1$) in both

CLLPS and EQLB, but the activity coefficient still increased from CLLPS to EQLB (Table S9). For pinic and pinonic acid, the deviation ($\gamma > 1$) was positive in CLLPS and its activity coefficient even larger in magnitude in EQLB such that the larger partitioning medium did not overcome the deviation in ideality resulting in the species being more abundant in the gas phase in EQLB compared to CLLPS. Interestingly, levoglucosan was the only species predicted to have an activity coefficient near 1 for the organic-rich (β) phase in EQLB calculations (Table S9). Due to the effect on the size of the partitioning medium resulting from additional species (specifically water and inorganic salts) in the β phase during EQLB, the effective C^* for levoglucosan was predicted to be 35% of its pure species value ($1.4 \mu\text{g m}^{-3}$, Table S8).

Predicted unfavorable interactions (limited miscibility within both the organic-rich and inorganic-rich liquid phases) resulted in pinonic acid (Figure 6f) being partitioned to the gas phase to a much greater degree than the measurements indicated. Model performance was consistent with previous work in which multiple measurement techniques showed slightly higher F_p than model predictions (Thompson et al., 2017). Formation of a second organic-rich phase (a third liquid phase) containing lower O:C compounds, which was not allowed in the AIOMFAC calculations, could improve pinonic acid partitioning predictions. The lack of a resolved hydrocarbon-like organic aerosol (HOA) component (Xu et al., 2015a) and representation of its associated functional groups in the model may have also contributed to an unfavorable environment for low O:C compounds.

Overall, the treatment of liquid phase mixing vs separation did not improve the mean bias in 2-methyltetrol predicted F_p . It also did not significantly change the mean error. The average fraction of 2-methyltetrols in the particles was represented fairly well by assuming half of the measured 2-methyltetrols are actually decomposition products of a fairly nonvolatile ($C^* = 10^{-6} \mu\text{g m}^{-3}$) dimer compound (dark grey square, Figure 5a,b). However, this assumption did not perform equally well at all times of day. Figure 6a indicates that the 50% dimer assumption leads to an underestimate in 2-methyltetrol F_p during the day and overestimate at night. Modeling 2-methyltetrols as entirely monomers with a pure species C^* of $8 \mu\text{g m}^{-3}$ at 298.15K (factor of 4.2 reduction in EVAPORATION predicted vapor pressure) reproduced the daytime 2-methyltetrol partitioning well, but overestimated partitioning to the particle at night. Even with the reduced P^{sat} (in the Adj Psat sensitivity), 2-methyltetrol monomers remained slightly more volatile than predicted by SIMPOL ($C^* = 5 \mu\text{g m}^{-3}$) at reference conditions. The average effective 2-methyltetrol C^* (accounting for the effects of temperature and partitioning medium) in the case of CLLPS was $6 \mu\text{g m}^{-3}$ while in the equilibrium calculations (EQLB) it was reduced further to $3.7 \mu\text{g m}^{-3}$ (Table S8). Thus, 2-methyltetrols behaved like compounds with an effective mean saturation concentration roughly half of the pure species value due to the influence of temperature and presence of other species in the particle.

4 Conclusions

In this work, conditions over the eastern United States were examined with a focus on gas-particle partitioning during the Southern Oxidant and Aerosol Study (SOAS). Different measurement techniques indicated fairly different ratios of ammonium to $2 \times$ total sulfate with the AMS instruments having the lowest values followed by CSN. The MARGA instrument (Allen et al., 2015) and SEARCH network indicated the highest ratios of ammonium to $2 \times$ sulfate of slightly less than 1 (mean of 0.8 to 0.9). ~~Thermodynamic~~ The lack of agreement of AMS and CSN data with thermodynamic models, but the agreement

5 between MARGA observations and models, indicates a potential bias in CSN measurements and that AMS data alone may not be suitable for thermodynamic modeling. The diversity in observational datasets can explain why some work has concluded thermodynamic models fail (Silvern et al., 2017) while others indicate models are adequate (Weber et al., 2016). This work finds thermodynamic equilibrium models (both ISORROPIA and AIOMFAC) are consistent with high ammonium to 2 × sulfate ratios in conjunction with about 70 to 80% of ammonia in the particle. Lower ammonium to sulfate ratios imply much higher fractions of total ammonia in the particle as thermodynamic equilibrium assumptions (and models) generally do not allow a large excess of gas-phase ammonia under highly acidic conditions. ~~To improve CMAQ predictions of ammonium to sulfate ratios and, therefore, pH needed for other aerosol processes such as isoprene-epoxydiol uptake (Pyc et al., 2013), model predictions of nonvolatile cations should be improved in conjunction with ammonia emissions.~~ While consideration of inorganics mixing in liquid phases with organic compounds may increase pH significantly compared to estimates from traditional models like ISORROPIA, that effect is likely not the cause of current inorganic aerosol model evaluation issues.

15 By performing ISORROPIA and AIOMFAC box modeling, this work demonstrates that our current thermodynamic understanding of ammonium and sulfate aerosol is consistent with (MARGA) observations in the southeastern U.S. atmosphere. Since models like CMAQ use the same thermodynamic basis, specifically ISORROPIA, these results build confidence that regional models can capture the thermodynamics of the ambient atmosphere. However, our results also demonstrate that for the partitioning of ammonia and ammonium to be correct, errors in emissions of nonvolatile cations, on the order of a factor of 3, must be resolved as well.

20 AIOMFAC-based predictions of gas-particle partitioning of organic compounds were sensitive to pure species vapor pressure estimates and predictions generally had a lower mean bias when EVAPORATION-based vapor pressures were adjusted downward by a factor of 4.2 and close to values estimated by SIMPOL for 2-methyltetrols, pinic acid, and hydroxyglutaric acid. AIOMFAC predicted organic compounds interact with significant amounts of water and inorganic ions. 2-methyltetrol predictions had roughly the same error in particle fraction (F_p) assuming 50% of measured particulate 2-methyltetrols were decomposition products or if their vapor pressure was adjusted downward by a factor of 4.2 (to $P^{\text{sat}}=1.4 \times 10^{-4}$ Pa at 298.15 K).

Code and data availability. CMAQ model code is available at <https://github.com/USEPA/CMAQ> and v5.2-gamma was used in this work.

ISORROPIA is available from <http://isorro피아.eas.gatech.edu/>.

AIOMFAC can be run online (<http://www.aiomfac.caltech.edu/>) or via contact with A. Zuend.

SOAS data is available at <https://esrl.noaa.gov/csd/groups/csd7/measurements/2013senex/>.

CSN data is available at <https://www.epa.gov/outdoor-air-quality-data>.

5 Model output associated with the final article will be available from the EPA Environmental Dataset Gateway at <https://edg.epa.gov/> if accepted.

Competing interests. The authors declare no competing interests.

Disclaimer. The US EPA through its Office of Research and Development supported the research described here. It has been subjected to Agency administrative review and approved for publication but may not necessarily reflect official Agency policy.

Acknowledgements. We thank J. Jimenez, G. Ruggeri, S. Takahama, and S. Lee for providing additional datasets that are summarized in the supporting information. We thank the CSN and SEARCH networks for providing long-term measurements. We thank two reviewers at EPA. We thank Paul Solomon for useful discussion. We thank CSRA for preparing emissions and meteorology input for CMAQ simulations. AZ was supported by the Natural Sciences and Engineering Research Council of Canada (NSERC), grant RGPIN/04315-2014. JLF acknowledges support from EPA-STAR RD-83539901. GIVW was supported by the NSF Graduate Research Fellowship (DGE 1106400). ~~Fp~~ F_p of organic compounds collected by SV-TAG at SOAS was supported by grants to UC Berkeley including NSF Atmospheric Chemistry Program 1250569 and Department of Energy SBIR grant DE-SC0004698. LX and NLN acknowledge support from National Science Foundation (NSF) Grant 1242258 and US Environmental Protection Agency (EPA) STAR Grant RD-83540301.

References

- Allen, H. M., Draper, D. C., Ayres, B. R., Ault, A., Bondy, A., Takahama, S., Modini, R. L., Baumann, K., Edgerton, E., Knote, C., Laskin, A., Wang, B., and Fry, J. L.: Influence of crustal dust and sea spray supermicron particle concentrations and acidity on inorganic NO_3^- aerosol during the 2013 Southern Oxidant and Aerosol Study, *Atmos. Chem. Phys.*, 15, 10669–10685, doi:10.5194/acp-15-10669-2015, 2015.
- Appel, K. W., Pouliot, G. A., Simon, H., Sarwar, G., Pye, H. O. T., Napelenok, S. L., Akhtar, F., and Roselle, S. J.: Evaluation of dust and trace metal estimates from the Community Multiscale Air Quality (CMAQ) model version 5.0, *Geosci. Model Dev.*, 6, 883–899, doi:10.5194/gmd-6-883-2013, 2013.
- 25 Bahreini, R., Ervens, B., Middlebrook, A. M., Warneke, C., de Gouw, J. A., DeCarlo, P. F., Jimenez, J. L., Brock, C. A., Neuman, J. A., Ryerson, T. B., Stark, H., Atlas, E., Brioude, J., Fried, A., Holloway, J. S., Peischl, J., Richter, D., Walega, J., Weibring, P., Wollny, A. G., and Fehsenfeld, F. C.: Organic aerosol formation in urban and industrial plumes near Houston and Dallas, Texas, *J. Geophys. Res.*, 114, n/a–n/a, doi:10.1029/2008JD011493, <http://dx.doi.org/10.1029/2008JD011493>, d00F16, 2009.
- Benner, C. L., Eatough, D. J., Eatough, N. L., and Bhardwaja, P.: Comparison of annular denuder and filter pack collection of $\text{HNO}_3(\text{g})$, $\text{HNO}_2(\text{g})$, $\text{SO}_2(\text{g})$, and particulate-phase nitrate, nitrite and sulfate in the south-west desert, *Atmos. Environ.*, 25, 1537–1545, doi:10.1016/0960-1686(91)90013-W, 1991.
- 30 Bertram, A. K., Martin, S. T., Hanna, S. J., Smith, M. L., Bodsworth, A., Chen, Q., Kuwata, M., Liu, A., You, Y., and Zorn, S. R.: Predicting the relative humidities of liquid-liquid phase separation, efflorescence, and deliquescence of mixed particles of ammonium sulfate, organic material, and water using the organic-to-sulfate mass ratio of the particle and the oxygen-to-carbon elemental ratio of the organic component, *Atmos. Chem. Phys.*, 11, 10995–11006, doi:10.5194/acp-11-10995-2011, 2011.
- 35 Budisulistiorini, S. H., Li, X., Bairai, S. T., Renfro, J., Liu, Y., Liu, Y. J., McKinney, K. A., Martin, S. T., McNeill, V. F., Pye, H. O. T., Nenes, A., Neff, M. E., Stone, E. A., Mueller, S., Knote, C., Shaw, S. L., Zhang, Z., Gold, A., and Surratt, J. D.: Examining the effects of anthropogenic emissions on isoprene-derived secondary organic aerosol formation during the 2013 Southern Oxidant and Aerosol Study (SOAS) at the Look Rock, Tennessee ground site, *Atmos. Chem. Phys.*, 15, 8871–8888, doi:10.5194/acp-15-8871-2015, 2015.
- 5 Budisulistiorini, S. H., Nenes, A., Carlton, A. G., Surratt, J. D., McNeill, V. F., and Pye, H. O. T.: Simulating aqueous-phase isoprene-epoxydiol (IEPOX) secondary organic aerosol production during the 2013 Southern Oxidant and Aerosol Study (SOAS), *Environ. Sci. Technol.*, 51, 5026–5034, doi:10.1021/acs.est.6b05750, 2017.
- Chan, M. N., Chan, A. W. H., Chhabra, P. S., Surratt, J. D., and Seinfeld, J. H.: Modeling of secondary organic aerosol yields from laboratory chamber data, *Atmos. Chem. Phys.*, 9, 5669–5680, doi:10.5194/acp-9-5669-2009, 2009.
- 10 Compernelle, S., Ceulemans, K., and Müller, J. F.: EVAPORATION: a new vapour pressure estimation method for organic molecules including non-additivity and intramolecular interactions, *Atmos. Chem. Phys.*, 11, 9431–9450, doi:10.5194/acp-11-9431-2011, 2011.
- Eddingsaas, N. C., VanderVelde, D. G., and Wennberg, P. O.: Kinetics and products of the acid-catalyzed ring-opening of atmospherically relevant butyl epoxy alcohols, *J. of Phys. Chem. A*, 114, 8106–8113, doi:10.1021/jp103907c, 2010.
- Edgerton, E. S., Hartsell, B. E., Saylor, R. D., Jansen, J. J., Hansen, D. A., and Hidy, G. M.: The Southeastern Aerosol Research and 15 Characterization Study: Part II. Filter-based measurements of fine and coarse particulate matter mass and composition, *J. Air Waste Manag. Assoc.*, 55, 1527–1542, 2005.

- Edgerton, E. S., Hartsell, B. E., Saylor, R. D., Jansen, J. J., Hansen, D. A., and Hidy, G. M.: The Southeastern Aerosol Research and Characterization Study, part 3: Continuous measurements of fine particulate matter mass and composition, *J. Air Waste Manag. Assoc.*, 56, 1325–1341, 2006.
- 20 Fang, T., Guo, H., Zeng, L., Verma, V., Nenes, A., and Weber, R. J.: Highly acidic ambient particles, soluble metals, and oxidative potential: a link between sulfate and aerosol toxicity, *Environ. Sci. Technol.*, 51, 2611–2620, doi:10.1021/acs.est.6b06151, 2017.
- Foroutan, H., Young, J., Napelenok, S., Ran, L., Appel, K. W., Gilliam, R. C., and Pleim, J. E.: Development and evaluation of a physics-based windblown dust emission scheme implemented in the CMAQ modeling system, *J. Adv. Model Earth Sy.*, 9, 585–608, doi:10.1002/2016MS000823, 2017.
- 25 Fountoukis, C. and Nenes, A.: ISORROPIA II: a computationally efficient thermodynamic equilibrium model for K^+ - Ca^{2+} - Mg^{2+} - NH_4^+ - Na^+ - SO_4^{2-} - NO_3^- - Cl^- - H_2O aerosols, *Atmos. Chem. and Phys.*, 7, 4639–4659, 2007.
- Goldstein, A. H. and Galbally, I. E.: Known and unexplored organic constituents in the Earth’s atmosphere, *Environ. Sci. Technol.*, 41, 1514–1521, doi:10.1021/es072476p, 2007.
- Guo, H.: Interactive comment on “The underappreciated role of nonvolatile cations on aerosol ammonium-sulfate molar ratios” by Hongyu Guo et al., *Atmos. Chem. Phys. Discuss.*, doi:10.5194/acp-2017-737-SC3, 2017.
- 30 Guo, H., Xu, L., Bougiatioti, A., Cerully, K. M., Capps, S. L., Hite Jr, J. R., Carlton, A. G., Lee, S. H., Bergin, M. H., Ng, N. L., Nenes, A., and Weber, R. J.: Fine-particle water and pH in the southeastern United States, *Atmos. Chem. Phys.*, 15, 5211–5228, doi:10.5194/acp-15-5211-2015, 2015.
- Guo, H., Liu, J., Froyd, K. D., Roberts, J. M., Veres, P. R., Hayes, P. L., Jimenez, J. L., Nenes, A., and Weber, R. J.: Fine particle pH and gas–particle phase partitioning of inorganic species in Pasadena, California, during the 2010 CalNex campaign, *Atmos. Chem. Phys.*, 17, 5703–5719, doi:10.5194/acp-17-5703-2017, 2017a.
- 35 Guo, H., Nenes, A., and Weber, R. J.: The underappreciated role of nonvolatile cations on aerosol ammonium-sulfate molar ratios, *Atmos. Chem. Phys. Discuss.*, 2017, 1–19, doi:10.5194/acp-2017-737, 2017b.
- Hansen, L. D., White, V. F., and Eatough, D. J.: Determination of gas-phase dimethyl sulfate and monomethyl sulfate, *Environ. Sci. Technol.*, 20, 872–878, doi:10.1021/es00151a004, 1986.
- 5 Heath, N. K., Pleim, J. E., Gilliam, R. C., and Kang, D.: A simple lightning assimilation technique for improving retrospective WRF simulations, *J. Adv. Model Earth Sys.*, 8, 1806–1824, doi:10.1002/2016MS000735, 2016.
- Hennigan, C. J., Izumi, J., Sullivan, A. P., Weber, R. J., and Nenes, A.: A critical evaluation of proxy methods used to estimate the acidity of atmospheric particles, *Atmos. Chem. Phys.*, 15, 2775–2790, doi:10.5194/acp-15-2775-2015, 2015.
- Hettiyadura, A. P. S., Jayarathne, T., Baumann, K., Goldstein, A. H., de Gouw, J. A., Koss, A., Keutsch, F. N., Skog, K., and Stone, E. A.: Qualitative and quantitative analysis of atmospheric organosulfates in Centreville, Alabama, *Atmos. Chem. and Phys.*, 17, 1343–1359, doi:10.5194/acp-17-1343-2017, 2017.
- 10 Hu, W., Palm, B. B., Day, D. A., Campuzano-Jost, P., Krechmer, J. E., Peng, Z., de Sá, S. S., Martin, S. T., Alexander, M. L., Baumann, K., Hacker, L., Kiendler-Scharr, A., Koss, A. R., de Gouw, J. A., Goldstein, A. H., Seco, R., Sjostedt, S. J., Park, J. H., Guenther, A. B., Kim, S., Canonaco, F., Prévôt, A. S. H., Brune, W. H., and Jimenez, J. L.: Volatility and lifetime against OH heterogeneous reaction of ambient isoprene-epoxydiols-derived secondary organic aerosol (IEPOX-SOA), *Atmos. Chem. Phys.*, 16, 11 563–11 580, doi:10.5194/acp-16-11563-2016, 2016.

- Hu, W., Campuzano-Jost, P., Day, D. A., Croteau, P., Canagaratna, M. R., Jayne, J. T., Worsnop, D. R., and Jimenez, J. L.: Evaluation of the new capture vaporizer for aerosol mass spectrometers (AMS) through field studies of inorganic species, *Aerosol Sci. Tech.*, 51, 735–754, doi:10.1080/02786826.2017.1296104, 2017.
- 20 Isaacman, G., Kreisberg, N. M., Yee, L. D., Worton, D. R., Chan, A. W. H., Moss, J. A., Hering, S. V., and Goldstein, A. H.: Online derivatization for hourly measurements of gas- and particle-phase semi-volatile oxygenated organic compounds by thermal desorption aerosol gas chromatography (SV-TAG), *Atmos. Meas. Tech.*, 7, 4417–4429, doi:10.5194/amt-7-4417-2014, 2014.
- Isaacman-VanWertz, G., Yee, L. D., Kreisberg, N. M., Wernis, R., Moss, J. A., Hering, S. V., de Sá, S. S., Martin, S. T., Alexander, M. L., Palm, B. B., Hu, W., Campuzano-Jost, P., Day, D. A., Jimenez, J. L., Riva, M., Surratt, J. D., Viegas, J., Manzi, A., Edgerton, E., Baumann, K., Souza, R., Artaxo, P., and Goldstein, A. H.: Ambient gas-particle partitioning of tracers for biogenic oxidation, *Environ. Sci. Technol.*, 50, 9952–9962, doi:10.1021/acs.est.6b01674, 2016.
- Johnson, D., Utembe, S. R., Jenkin, M. E., Derwent, R. G., Hayman, G. D., Alfarra, M. R., Coe, H., and McFiggans, G.: Simulating regional scale secondary organic aerosol formation during the TORCH 2003 campaign in the southern UK, *Atmos. Chem. Phys.*, 6, 403–418, doi:10.5194/acp-6-403-2006, 2006.
- 30 Kwamena, N. O. A., Buajarnern, J., and Reid, J. P.: Equilibrium morphology of mixed organic/inorganic/aqueous aerosol droplets: investigating the effect of relative humidity and surfactants, *J. Phys. Chem. A*, 114, 5787–5795, doi:10.1021/jp1003648, 2010.
- Lopez-Hilfiker, F. D., Mohr, C., D’Ambro, E. L., Lutz, A., Riedel, T. P., Gaston, C. J., Iyer, S., Zhang, Z., Gold, A., Surratt, J. D., Lee, B. H., Kurten, T., Hu, W. W., Jimenez, J., Hallquist, M., and Thornton, J. A.: Molecular composition and volatility of organic aerosol in the southeastern U.S.: implications for IEPOX derived SOA, *Environ. Sci. Technol.*, 50, 2200–2209, doi:10.1021/acs.est.5b04769, 2016.
- 35 Middlebrook, A. M., Bahreini, R., Jimenez, J. L., and Canagaratna, M. R.: Evaluation of composition-dependent collection efficiencies for the Aerodyne Aerosol Mass Spectrometer using field data, *Aerosol Sci. Technol.*, 46, 258–271, doi:10.1080/02786826.2011.620041, 2012.
- Nenes, A., Pandis, S. N., and Pilinis, C.: ISORROPIA: A new thermodynamic equilibrium model for multiphase multicomponent inorganic aerosols, *Aquat. Geochem.*, 4, 123–152, doi:10.1023/A:1009604003981, 1998.
- Nolte, C. G., Appel, K. W., Kelly, J. T., Bhave, P. V., Fahey, K. M., Collett Jr, J. L., Zhang, L., and Young, J. O.: Evaluation of the Community Multiscale Air Quality (CMAQ) model v5.0 against size-resolved measurements of inorganic particle composition across sites in North America, *Geosci. Model Dev.*, 8, 2877–2892, doi:10.5194/gmd-8-2877-2015, 2015.
- 5 O’Meara, S., Booth, A. M., Barley, M. H., Topping, D., and McFiggans, G.: An assessment of vapour pressure estimation methods, *Phys. Chem. Chem. Phys.*, 16, 19453–19469, doi:10.1039/C4CP00857J, 2014.
- Otte, T. L. and Pleim, J. E.: The Meteorology-Chemistry Interface Processor (MCIP) for the CMAQ modeling system: Updates through MCIPv3.4.1, *Geosci. Model Dev.*, 3, 243–256, 2010.
- Pankow, J. F. and Asher, W. E.: SIMPOL.1: a simple group contribution method for predicting vapor pressures and enthalpies of vaporization of multifunctional organic compounds, *Atmos. Chem. Phys.*, 8, 2773–2796, doi:10.5194/acp-8-2773-2008, 2008.
- 10 Pleim, J. E., Bash, J. O., Walker, J. T., and Cooter, E. J.: Development and evaluation of an ammonia bidirectional flux parameterization for air quality models, *J. Geophys. Res.*, 118, 3794–3806, doi:10.1002/jgrd.50262, 2013.
- Pye, H. O. T., Pinder, R. W., Piletic, I. R., Xie, Y., Capps, S. L., Lin, Y.-H., Surratt, J. D., Zhang, Z., Gold, A., Luecken, D. J., Hutzell, W. T., Jaoui, M., Offenberg, J. H., Kleindienst, T. E., Lewandowski, M., and Edney, E. O.: Epoxide pathways improve model predictions of isoprene markers and reveal key role of acidity in aerosol formation, *Environ. Sci. Technol.*, 47, 11056–11064, doi:10.1021/es402106h, 2013.
- 15

- 20 Pye, H. O. T., Murphy, B. N., Xu, L., Ng, N. L., Carlton, A. G., Guo, H., Weber, R., Vasilakos, P., Appel, K. W., Budisulistiorini, S. H., Surratt, J. D., Nenes, A., Hu, W., Jimenez, J. L., Isaacman-VanWertz, G., Misztal, P. K., and Goldstein, A. H.: On the implications of aerosol liquid water and phase separation for organic aerosol mass, *Atmos. Chem. Phys.*, 17, 343–369, doi:10.5194/acp-17-343-2017, 2017.
- Reff, A., Bhave, P. V., Simon, H., Pace, T. G., Pouliot, G. A., Mobley, J. D., and Houyoux, M.: Emissions inventory of PM_{2.5} trace elements across the United States, *Environ. Sci. Technol.*, 43, 5790–5796, doi:10.1021/es802930x, 2009.
- Reid, J. P., Dennis-Smith, B. J., Kwamena, N.-O. A., Miles, R. E. H., Hanford, K. L., and Homer, C. J.: The morphology of aerosol particles consisting of hydrophobic and hydrophilic phases: hydrocarbons, alcohols and fatty acids as the hydrophobic component, *Phys. Chem. Chem. Phys.*, 13, 15 559–15 572, doi:10.1039/C1CP21510H, 2011.
- Renbaum-Wolff, L., Grayson, J. W., Bateman, A. P., Kuwata, M., Sellier, M., Murray, B. J., Shilling, J. E., Martin, S. T., and Bertram, A. K.: Viscosity of alpha-pinene secondary organic material and implications for particle growth and reactivity, *P. Natl. Acad. Sci. USA*, 110, 8014–8019, doi:10.1073/pnas.1219548110, 2013.
- 30 Rindelaub, J. D., Craig, R. L., Nandy, L., Bondy, A. L., Dutcher, C. S., Shepson, P. B., and Ault, A. P.: Direct measurement of pH in individual particles via Raman microspectroscopy and variation in acidity with relative humidity, *J. of Phys Chem. A*, 120, 911–917, doi:10.1021/acs.jpca.5b12699, 2016.
- Silvern, R. F., Jacob, D. J., Kim, P. S., Marais, E. A., Turner, J. R., Campuzano-Jost, P., and Jimenez, J. L.: Inconsistency of ammonium–sulfate aerosol ratios with thermodynamic models in the eastern US: a possible role of organic aerosol, *Atmos. Chem. Phys.*, 17, 5107–5118, doi:10.5194/acp-17-5107-2017, 2017.
- 35 Solomon, P. A., Mitchell, W., Tolocka, M., Norris, G., Gemmill, D., Wiener, R., Vanderpool, R., Murdoch, R., Natarajan, S., and Hardison, E.: Evaluation of PM_{2.5} chemical speciation samplers for use in the EPA National PM_{2.5} Chemical Speciation Network, Report EPA-454/R-01-005, United States Environmental Protection Agency, 2000.
- Solomon, P. A., Crumpler, D., Flanagan, J. B., Jayanty, R. K. M., Rickman, E. E., and McDade, C. E.: U.S. National PM_{2.5} Chemical Speciation Monitoring Networks—CSN and IMPROVE: Description of networks, *J. Air Waste Manag. Assoc.*, 64, 1410–1438, doi:10.1080/10962247.2014.956904, 2014.
- Song, M., Marcolli, C., Krieger, U. K., Zuend, A., and Peter, T.: Liquid-liquid phase separation in aerosol particles: Dependence on O:C, organic functionalities, and compositional complexity, *Geophys. Res. Lett.*, 39, L19 801, doi:10.1029/2012GL052807, 2012.
- 5 Song, M., Marcolli, C., Krieger, U. K., Lienhard, D. M., and Peter, T.: Morphologies of mixed organic/inorganic/aqueous aerosol droplets, *Faraday Discuss.*, 165, 289–316, doi:10.1039/C3FD00049D, 2013.
- Stockdale, A., Krom, M. D., Mortimer, R. J. G., Benning, L. G., Carslaw, K. S., Herbert, R. J., Shi, Z., Myriokefalitakis, S., Kanakidou, M., and Nenes, A.: Understanding the nature of atmospheric acid processing of mineral dusts in supplying bioavailable phosphorus to the oceans, *P. Natl. Acad. Sci. USA*, 113, 14 639–14 644, doi:10.1073/pnas.1608136113, 2016.
- 10 Thompson, S. L., Yatavelli, R. L. N., Stark, H., Kimmel, J. R., Krechmer, J. E., Day, D. A., Hu, W., Isaacman-VanWertz, G., Yee, L., Goldstein, A. H., Khan, M. A. H., Holzinger, R., Kreisberg, N., Lopez-Hilfiker, F. D., Mohr, C., Thornton, J. A., Jayne, J. T., Canagaratna, M., Worsnop, D. R., and Jimenez, J. L.: Field intercomparison of the gas/particle partitioning of oxygenated organics during the Southern Oxidant and Aerosol Study (SOAS) in 2013, *Aerosol Sci. Technol.*, 51, 30–56, doi:10.1080/02786826.2016.1254719, 2017.
- Topping, D., Barley, M., Bane, M. K., Higham, N., Aumont, B., Dingle, N., and McFiggans, G.: UManSysProp v1.0: an online and open-source facility for molecular property prediction and atmospheric aerosol calculations, *Geosci. Model Dev.*, 9, 899–914, doi:10.5194/gmd-9-899-2016, 2016.

- Weber, R. J., Guo, H., Russell, A. G., and Nenes, A.: High aerosol acidity despite declining atmospheric sulfate concentrations over the past 15 years, *Nature Geosci.*, 9, 282–285, doi:10.1038/ngeo2665 <http://www.nature.com/ngeo/journal/v9/n4/abs/ngeo2665.html#supplementary-information>, 2016.
- 20 Xu, L., Guo, H., Boyd, C. M., Klein, M., Bougiatioti, A., Cerully, K. M., Hite, J. R., Isaacman-VanWertz, G., Kreisberg, N. M., Knote, C., Olson, K., Koss, A., Goldstein, A. H., Hering, S. V., de Gouw, J., Baumann, K., Lee, S.-H., Nenes, A., Weber, R. J., and Ng, N. L.: Effects of anthropogenic emissions on aerosol formation from isoprene and monoterpenes in the southeastern United States, *P. Natl. Acad. Sci. USA*, 112, 37–42, doi:10.1073/pnas.1417609112, 2015a.
- Xu, L., Suresh, S., Guo, H., Weber, R. J., and Ng, N. L.: Aerosol characterization over the southeastern United States using high-resolution
25 aerosol mass spectrometry: spatial and seasonal variation of aerosol composition and sources with a focus on organic nitrates, *Atmos. Chem. Phys.*, 15, 7307–7336, doi:10.5194/acp-15-7307-2015, 2015b.
- Xu, L., Guo, H., Weber, R. J., and Ng, N. L.: Chemical characterization of water-soluble organic aerosol in contrasting rural and urban environments in the southeastern United States, *Environ. Sci. Technol.*, 51, 78–88, doi:10.1021/acs.est.6b05002, 2017.
- You, Y., Renbaum-Wolff, L., and Bertram, A. K.: Liquid-liquid phase separation in particles containing organics mixed with ammonium
30 sulfate, ammonium bisulfate, ammonium nitrate or sodium chloride, *Atmos. Chem. Phys.*, 13, 11 723–11 734, doi:10.5194/acp-13-11723-2013, 2013.
- 625 Yu, X.-Y., Lee, T., Ayres, B., Kreidenweis, S. M., Malm, W., and Collett Jr, J. L.: Loss of fine particle ammonium from denuded nylon filters, *Atmos. Environ.*, 40, 4797–4807, doi:<https://doi.org/10.1016/j.atmosenv.2006.03.061>, 2006.
- Zuend, A. and Seinfeld, J. H.: Modeling the gas-particle partitioning of secondary organic aerosol: the importance of liquid-liquid phase separation, *Atmos. Chem. Phys.*, 12, 3857–3882, doi:10.5194/acp-12-3857-2012, 2012.
- Zuend, A. and Seinfeld, J. H.: A practical method for the calculation of liquid-liquid equilibria in multicomponent organic-water-electrolyte
630 systems using physicochemical constraints, *Fluid Phase Equilibr.*, 337, 201–213, doi:10.1016/j.fluid.2012.09.034, 2013.
- Zuend, A., Marcolli, C., Luo, B. P., and Peter, T.: A thermodynamic model of mixed organic-inorganic aerosols to predict activity coefficients, *Atmos. Chem. Phys.*, 8, 4559–4593, doi:10.5194/acp-8-4559-2008, 2008.
- Zuend, A., Marcolli, C., Peter, T., and Seinfeld, J. H.: Computation of liquid-liquid equilibria and phase stabilities: implications for RH-
635 dependent gas/particle partitioning of organic-inorganic aerosols, *Atmos. Chem. Phys.*, 10, 7795–7820, doi:10.5194/acp-10-7795-2010, 2010.
- Zuend, A., Marcolli, C., Booth, A. M., Lienhard, D. M., Soonsin, V., Krieger, U. K., Topping, D. O., McFiggans, G., Peter, T., and Seinfeld, J. H.: New and extended parameterization of the thermodynamic model AIOMFAC: calculation of activity coefficients for organic-inorganic mixtures containing carboxyl, hydroxyl, carbonyl, ether, ester, alkenyl, alkyl, and aromatic functional groups, *Atmos. Chem. and Phys.*, 11, 9155–9206, 2011.

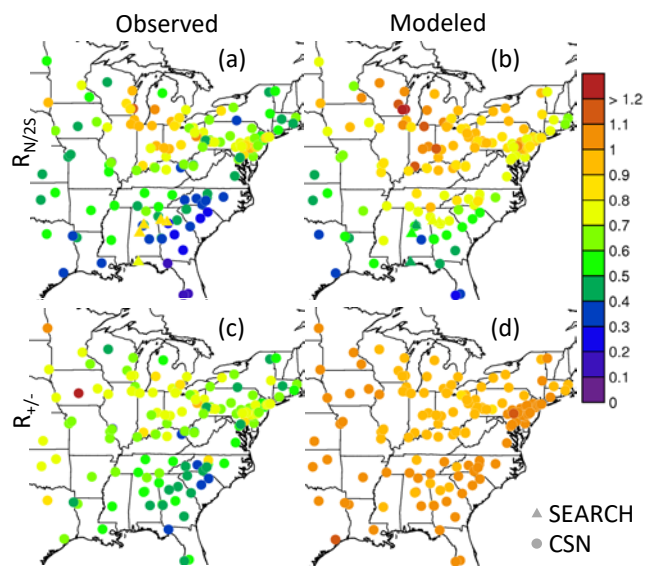


Figure 1. Molar ratio of aerosol ammonium to $2\times$ sulfate ($R_{N/2S}$) (a-b) and cations to anions ($R_{+/-}$) (c-d) over the eastern US for June 1- July 15, 2013 based on observations and predicted by the CMAQ model.

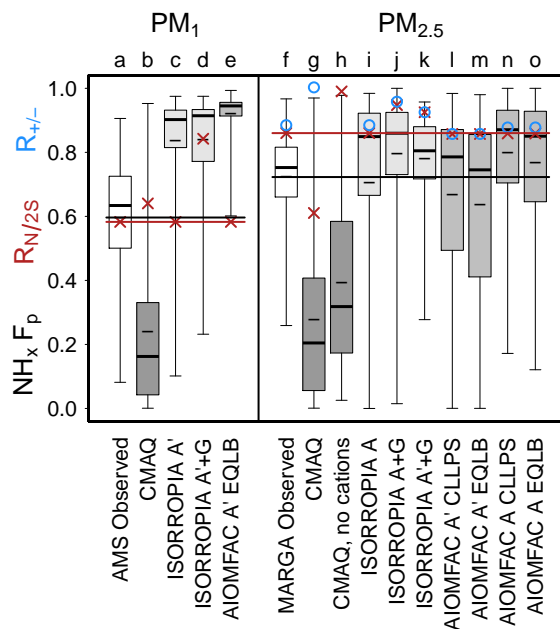


Figure 2. Gas-particle partitioning of ammonia ($\text{NH}_x \text{F}_p = \text{ammonium}/(\text{ammonia}+\text{ammonium})$), mean $R_{N/2S}$ (red \times), and mean $R_{+/-}$ (blue \circ) for $\text{PM}_{1.0}$ measured by the Georgia Tech AMS (Xu et al., 2015a) and $\text{PM}_{2.5}$ measured by a MARGA (Allen et al., 2015) as well as predicted by a CMAQ regional chemical transport model calculation and box models for SOAS conditions at CTR. F_p boxplots indicate the maximum, 75th percentile, median, 25th percentile, and minimum. Short dashes within the boxplots indicate the mean F_p . Box model inputs were either the aerosol (A) or aerosol and gas concentrations (A+G). Box models were run with either the ammonium-sulfate system (A') or including all cations and anions (A). AIOMFAC calculations assumed complete liquid-liquid phase separation between the organic-rich and electrolyte-rich phases (CLLPS) or employed a full equilibrium calculation with organic compounds in which phase separation was calculated based on composition (EQLB). Observed gas-phase ammonia concentrations are from the SEARCH network at CTR. Boxplots are labeled by a letter for easier reference in the text. Shading of the boxplot interquartile range distinguishes different models (CMAQ, ISORROPIA, and AIOMFAC). The horizontal lines correspond to mean observed $\text{NH}_x \text{F}_p$ (black) and $R_{N/2S}$ (red). A simulation is consistent with observations if it reproduces both $\text{NH}_x \text{F}_p$ and $R_{N/2S}$.

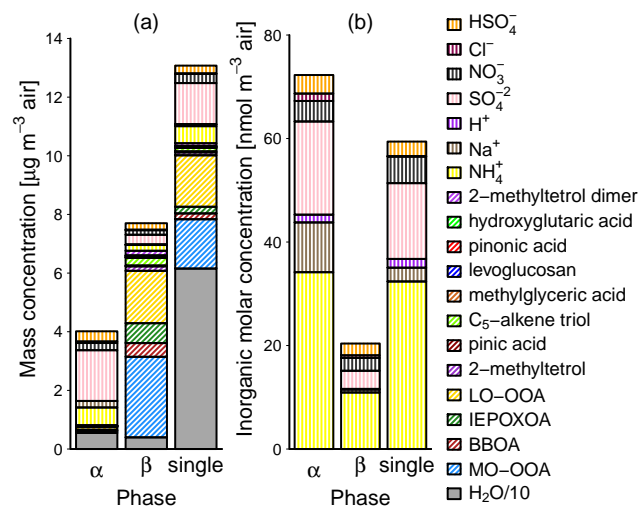


Figure 3. Average composition of the α (electrolyte-rich), β (organic-rich), and single phase in terms of (a) mass (organic and inorganic components) and (b) moles (ions only) predicted by AIOMFAC using $\text{PM}_{2.5}$ aerosol composition observed during SOAS. Species are stacked in the same order as indicated by the legend.

Table 1. $[\text{H}^+]_{\text{air}}$ and pH predicted for $\text{PM}_{2.5}$ at SOAS CTR (median \pm one standard deviation) under conditions of complete liquid-liquid phase separation between the organic-rich and electrolyte-rich phases (CLLPS) or in a full equilibrium calculation in which phase separation was calculated based on composition (EQLB).

Model	CLLPS	EQLB
$[\text{H}^+]_{\text{air}}$ in nmol m^{-3} air		
AIOMFAC (A')	1.9 ± 1.9	1.3 ± 1.6
AIOMFAC (A)	1.8 ± 2.1	1.1 ± 1.8
ISORROPIA (A)	2.0 ± 2.8	NA
ISORROPIA (A+G)	0.5 ± 1.5	NA
$pH = -\log_{10}(\gamma_{\text{H}^+}[\text{H}^+]_{\text{air}}/[S])$		
AIOMFAC (A')	1.3 ± 1.2	1.4 ± 1.2
AIOMFAC (A)	1.3 ± 2.1	1.5 ± 2.0
ISORROPIA (A)	0.7 ± 2.5	NA
ISORROPIA (A+G)	1.1 ± 0.7	NA

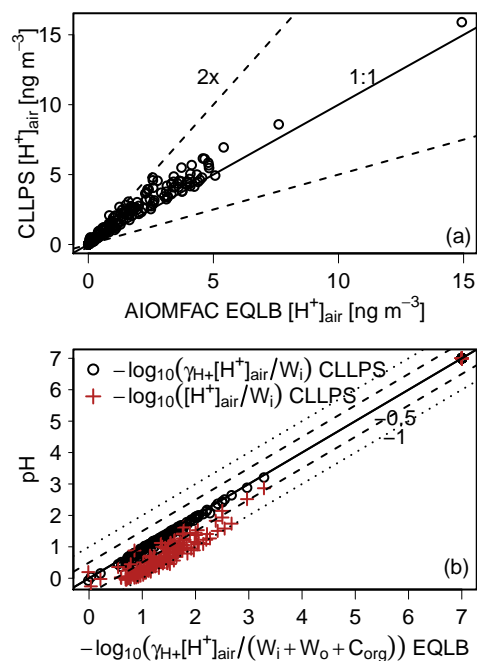


Figure 4. (a) $[H^+]_{air}$ and (b) pH predicted for PM_{2.5} using AIOMFAC. Dashed lines in panel (a) indicate a factor of two difference from the 1:1 line. Dashed lines in (b) represent a ± 0.5 shift in pH while dotted lines represent a ± 1 shift in pH. Series marked in open circles (○) are summarized in Table 1. All calculations used the ammonium-sodium-sulfate-nitrate-chloride and organic compounds system.

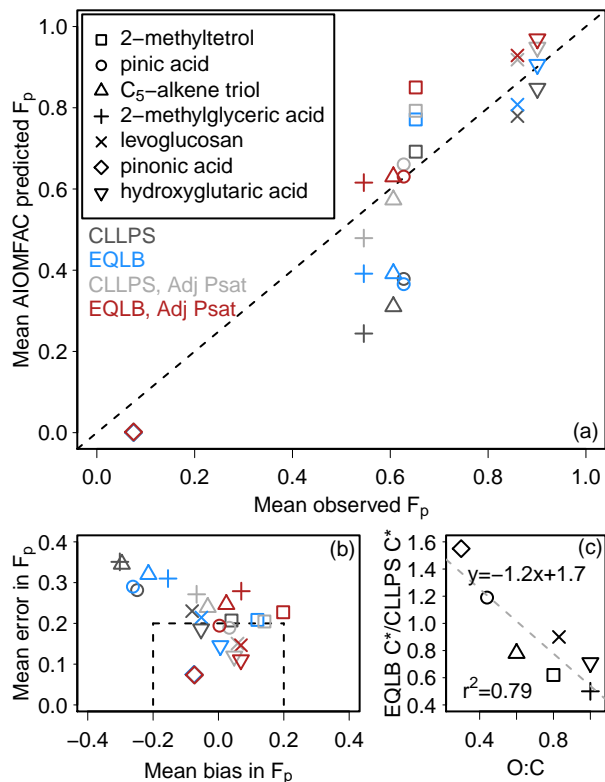


Figure 5. Observed and AIOMFAC-based predictions of equilibrium partitioning of organic compounds in the presence of MARGA-measured $PM_{2.5}$ inorganics. In panel (b), mean bias = $\frac{1}{n} \sum_{i=1}^n (M_i - O_i)$ and mean error = $\frac{1}{n} \sum_{i=1}^n |M_i - O_i|$ where M_i is the model prediction and O_i is the observation of F_p . The ratio of mean saturation concentration under EQLB compared to CLLPS conditions (c) uses predictions from the adjusted vapor pressure calculations (Adj Psat). Modeled particulate 2-methyltetrols are 50% dimers except with Adj Psat.

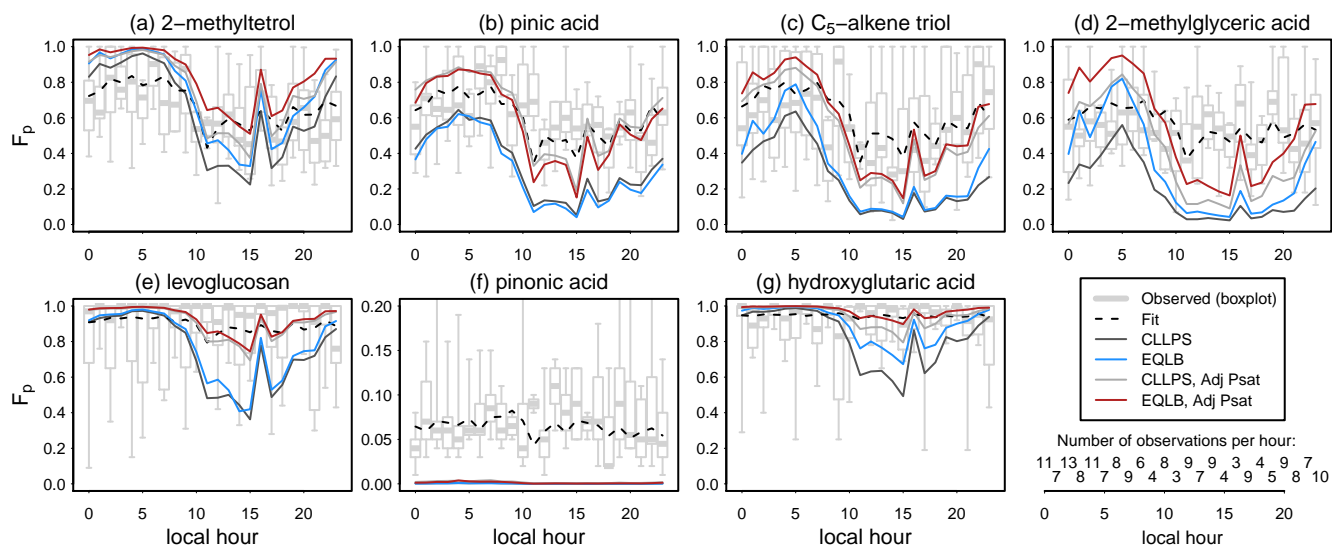


Figure 6. Fraction of each explicit organic species in the particle as a function of hour of day between 1 June and 15 July 2013 at CTR. 2-methyltetrols were modeled as 50% dimers in the particle for CLLPS and EQLB. When the pure species vapor pressure was adjusted, 2-methyltetrols were assumed to be entirely monomers. Fit is based on traditional absorptive partitioning to an organic compounds-only phase (Equation S1).

Supporting Information for:

Coupling of organic and inorganic aerosol systems and the
effect on gas-particle partitioning in the southeastern United States

Havala O. T. Pye¹, Andreas Zuend², Juliane L. Fry³, Gabriel Isaacman-VanWertz^{4,5},
Shannon L. Capps⁶, K. Wyatt Appel¹, Hosein Foroutan¹, Lu Xu⁷, Nga L. Ng^{8,9}, and Allen H. Goldstein^{5,10}

¹National Exposure Research Laboratory, US Environmental Protection Agency, Research Triangle Park,
North Carolina, USA

²Department of Atmospheric and Oceanic Sciences, McGill University, Montreal, Quebec, CAN

³Department of Chemistry, Reed College, Portland, Oregon, USA

⁴Department of Civil and Environmental Engineering, Virginia Polytechnic Institute and State University,
Blacksburg, Virginia, USA

⁵Department of Environmental Science, Policy, and Management, University of California, Berkeley,
California, USA

⁶Civil, Architectural, and Environmental Engineering, Drexel University, Philadelphia, Pennsylvania,
USA

⁷Department of Environmental Science and Engineering, California Institute of Technology, Pasadena,
California, USA

⁸School of Chemical and Biomolecular Engineering, Georgia Institute of Technology, Atlanta, GA, USA

⁹School of Earth and Atmospheric Sciences, Georgia Institute of Technology, Atlanta, Georgia, USA

¹⁰Department of Civil and Environmental Engineering, University of California, Berkeley, California,
USA

Correspondence to: Havala O. T. Pye (pye.havala@epa.gov)

Includes: 18 pages
9 tables
10 figures

Table S1: Functional group assignments of organic compounds and factors used as species in AIOMFAC. AIOMFAC does not include experimentally-constrained interaction parameters for the bisulfate anion with ester, aldehyde, ketone, or aromatic carbon-alcohol functional groups (Zuend and Seinfeld, 2012), although an analogy approach can be employed to estimate these interactions. In addition, organonitrate -- ion interaction parameters are not yet available. When needed, these functional groups were assigned to another representative group. Isoprene-OA used in AIOMFAC consisted of measured Isoprene-OA minus explicitly represented isoprene-derived compounds. LO-OOA used in AIOMFAC consisted of measured LO-OOA minus explicitly represented monoterpene-derived compounds. BBOA used in AIOMFAC consisted of measured BBOA minus levoglucosan. For AMS PMF factors, functional group assignments were made by selecting a compound representative of the factor (levoglucosan for BBOA, 2-methyltetrol dimer for Isoprene-OA, C₈O₄H₁₄ for LO-OOA, and fulvic acid for MO-OOA) and adjusting the functional groups up or down to result in an overall O:C and H:C more consistent with the PMF factor. Molecular masses were kept below 500 g mol⁻¹. All compound/factor concentrations were set ≥ zero and the total mass normalized to reproduce total organic aerosol mass measured by the GT AMS.

AIOMFAC Functional Groups		Number of Functional Groups in Organic Species															
Group Name	Group molecular weight (g/mol)	Number of C in group	Number of O in group	Number of H in group	MO-OOA	BBOA	2-methyltetrol dimer	Isoprene-OA	LO-OOA	2-methyltetrol	Pinic acid	C5-alkane triol	2-methylglyceric acid	levoglucosan	Pinonic acid	Hydroxyglutaric acid	
alkyl (standard)	(CH3)	15	1	0	3	0	0	1	2	2	0	2	1	1	0	3	0
	(CH2)	14	1	0	2	2	1	0	1	1	0	2	0	0	0	2	2
	(CH)	13	1	0	1	0	1	0	1	1	0	2	0	0	1	2	0
	(C)	12	1	0	0	0	0	1	1	0	0	1	0	0	0	1	0
alkyl in alcohols	(CH3[alc])	15	1	0	3	0	0	1	0	0	1	0	0	0	0	0	0
	(CH2[alc])	14	1	0	2	0	0	0	0	0	0	0	0	0	0	0	0
	(CH[alc])	13	1	0	1	0	0	0	0	0	0	0	0	0	0	0	0
	(C[alc])	12	1	0	0	0	0	0	0	0	0	0	0	0	0	0	0
alkyl in tail of alcohols	(CH3[alc-tail])	15	1	0	3	0	0	0	0	0	0	0	0	0	0	0	0
	(CH2[alc-tail])	14	1	0	2	0	0	0	0	0	0	0	0	0	0	0	0
	(CH[alc-tail])	13	1	0	1	0	0	0	0	0	0	0	0	0	0	0	0
	(C[alc-tail])	12	1	0	0	0	0	0	0	0	0	0	0	0	0	0	0
alkyl bonded to OH (OH separately)	(CH3[OH])	15	1	0	3	0	0	0	0	0	0	0	0	0	0	0	0
	(CH2[OH])	14	1	0	2	1	0	3	1	2	2	0	2	1	0	0	0
	(CH[OH])	13	1	0	1	3	2	2	1	1	1	0	0	0	3	1	1
	(C[OH])	12	1	0	0	4	0	1	0	1	1	0	0	1	0	0	0
alkenyl	(CH2=CH)	27	2	0	3	0	0	0	0	0	0	0	0	0	0	0	0
	(CH=CH)	26	2	0	2	0	0	0	0	0	0	0	0	0	0	0	0
	(CH2=C)	26	2	0	2	0	0	0	0	0	0	0	0	0	0	0	0

	(CH=C)	25	2	0	1	0	0	0	0	0	0	0	0	0	0	0	0
	(C=C)	24	2	0	0	0	0	0	0	0	0	0	0	0	0	0	0
aromatic hydro-carbon	(ACH)	13	1	0	1	0	0	0	0	0	0	0	0	0	0	0	0
	(AC)	12	1	0	0	0	0	0	0	0	0	0	2	0	0	0	0
aromatic carbon-alcohol	(ACOH)	29	1	1	1	0	0	0	0	0	0	0	0	0	0	0	0
hydroxyl	(OH)	17	0	1	1	8	2	6	2	4	4	0	3	2	3	1	1
carboxyl	(COOH)	45	1	2	1	2	0	0	2	0	0	2	0	1	0	1	2
	(HCOOH)	46	1	2	2	0	0	0	0	0	0	0	0	0	0	0	0
ketone	(CH3CO)	43	2	1	3	0	0	0	0	0	0	0	0	0	0	0	0
	(CH2CO)	42	2	1	2	0	0	0	0	0	0	0	0	0	0	0	0
aldehyde	(CHO [aldehyde])	29	1	1	1	0	0	0	0	0	0	0	0	0	0	0	0
ester	(CH3 COO)	59	2	2	3	0	0	0	0	0	0	0	0	0	0	0	0
	(CH2 COO)	58	2	2	2	0	0	0	0	0	0	0	0	0	0	0	0
ether	(CH3O)	31	1	1	3	0	0	0	0	0	0	0	0	0	0	0	0
	(CH2O)	30	1	1	2	1	1	1	1	0	0	0	0	0	1	0	0
	(CHO [ether])	29	1	1	1	1	1	0	0	0	0	0	0	1	0	0	0

Table S2: Properties of AIOMFAC surrogates.

	MO-OOA	BBOA	2-methyltetrol dimer	Isoprene-OA	LO-OOA	2-methyltetrol	Pinic acid	C5-alkene triol	2-methylglyceric acid	Levogluconan	Pinonic acid	Hydroxyglutaric acid
Molecular weight (g/mol)	414	146	254	250	178	136	186	118	120	162	186	148
O:C	1.00	0.67	0.70	0.70	0.50	0.80	0.44	0.60	1.00	0.83	0.30	1.00
H:C	1.57	1.67	2.20	1.80	2.25	2.40	1.56	2.00	2.00	1.67	1.80	1.60
OM/OC	2.46	2.03	2.12	2.08	1.85	2.27	1.72	1.97	2.50	2.25	1.55	2.47

Table S3: SMILES strings for organic compounds and factors.

Model Species	SMILES representation
MO-OOA	<chem>C1(C(C(C(C2C1C(C3(C(O2)(C(C(OC3)(CO)O)O)O)=O)O)O)(C(=O)O)O</chem>
BBOA	<chem>C1C2C(CC(C(O1)O2)O)O</chem>
Isoprene-OA	<chem>C(=O)(O)C(C)C(O)COC(C)(CO)CC(=O)O</chem>
LO-OOA	<chem>CC(C)CC(O)(CO)C(O)CO</chem>
2-methyltetrol (monomer)	<chem>C(O)C(O)(C)C(O)CO</chem>
Pinic acid	<chem>CC1(C(CC1C(=O)O)CC(=O)O)C</chem>
C5-alkene triol	<chem>C(O)C(C)=C(O)CO</chem>
2-methylglyceric acid	<chem>CC(CO)(C(=O)O)O</chem>
Levogluconan	<chem>C1C2C(C(C(C(O1)O2)O)O)O</chem>
Pinonic acid	<chem>CC(=O)C1CC(C1(C)C)CC(=O)O</chem>
Hydroxyglutaric acid	<chem>C(CC(=O)O)C(C(=O)O)O</chem>
2-methyltetrol dimer	<chem>OCC(O)(C)C(O)COC(CO)(C)C(O)CO</chem>

Table S4: Saturation concentrations at $T_{ref}=298.15$ K and enthalpies of vaporization (ΔH in kJ/mol) for 298.15 ± 7 K fitted to reproduce ambient partitioning or predicted based on vapor pressure for the pure species. Fitted values are based on traditional absorptive partitioning to an organic-only medium:

$$F_{p,i} = (1 + T_{ref}/T \times \exp[\Delta H/8314 \text{ kJ}^{-1} \text{ mol K} \times (1/T_{ref} - 1/T) \text{ 1/K}] \times C^* / (M_i \times N))^{-1} \quad (S1)$$

where M_i is the molecular mass of the species and $N = C_{org}/200 \text{ g mol}^{-1}$. EVAPORATION, MYN, and NN structure-based estimates are provided by UMANSYSPROP (Topping et al., 2016) available at <http://umansysprop.seaes.manchester.ac.uk>. Lower and upper bound parameter estimates are provided for the 95% confidence interval of the fits to ambient data. NS indicates the parameter was not statistically significant in the fit. AIOMFAC adjusted C^* reflect base values multiplied by 0.238 (Adj Psat sensitivity calculations).

	2-methyltetrol (monomer)	2-methyltetrol dimer	C5-alkene triol	2-methylglyceric acid	pinic acid	pinonic acid	hydroxyglutaric acid	levoglucosan
C^* ($\mu\text{g m}^{-3}$)								
SIMPOL ^a	5	6.6E-07	565	4899	7	980	2	16
EVAPORATION ^b	34	2.8E-06	63	301	22	7213	9	18
MYN ^c	507	2.1E-01	7217	2594	1051	18366	152	8172
NN ^d	10	5.8E-08	1205	115	53	4556	1	269
Fit to Ambient	1.8	NA	2.1	2.7	3.5	81	0.2	0.5
Fit to Ambient (lower bound)	1.5	NA	1.7	2.3	3.0	70	0.2	0.4
Fit to Ambient (upper bound)	2.1	NA	2.5	3.2	4.2	94	0.3	0.7
AIOMFAC Adjusted (Adj Psat)	7.7	NA	14	69	5.1	1700	2	4
ΔH^{vap} (kJ mol^{-1})								
SIMPOL	107	167	89	78	99	76	102	98
EVAPORATION	107	176	105	97	112	89	112	115
MYN	92	120	83	86	88	78	95	81
NN	117	211	94	106	108	87	127	103
Fit to Ambient	122	NA	129	71	120	NS	NS	NS
Fit to Ambient (lower bound)	87	NA	84	35	84	NS	NS	NS
Fit to Ambient (upper bound)	158	NA	178	108	158	NS	NS	NS

^aSIMPOL: Pankow and Asher (2008)

^bEVAPORATION: Compernelle et al. (2011). Used with AIOMFAC.

^cMYN: Myrdal and Yalkowsky (1997) vapor pressure method with Nannoolal et al. (2004) boiling point method.

^dNN: Nannoolal et al. (2008) vapor pressure method with Nannoolal et al. (2004) boiling point method.

Table S5: Average concentrations of particulate ammonium and sulfate and their ratios at the SOAS Centreville site from 1 June 2013 to 15 July 2013.

Instrument	Number of Hourly Aggregated Observations	Mean Ammonium ($\mu\text{g m}^{-3}$)	Mean Sulfate ($\mu\text{g m}^{-3}$)	$R_{N/2S}$ Molar Ratio of Means	Mean of Molar Ratio $R_{N/2S}$
GT AMS (Xu et al. 2015a,b) PM_{10}	881	0.40	1.8	0.59	0.51
CU AMS (Hu et al. 2015) PM_{10}	646	0.39	2.2	0.47	0.44
SEARCH CTR $\text{PM}_{2.5}$	739	0.59	1.8	0.86	0.96
MARGA (Allen et al. 2015) $\text{PM}_{2.5}$	948	0.67	2.2	0.81	0.80
URG Corporation Ambient Ion Monitor (AIM) 9000-D PM_{10} & $\text{PM}_{2.5}$	374	0.91	2.1	1.2	1.4

Table S6: Molar ratio of ammonium to sulfate ($R_{N/S}$) from Silvern et al. (2017) and resulting $R_{N/2S}$.

Dataset	$R_{N/S}$	$R_{N/2S}$
Eastern US CSN Summer 2013 $\text{PM}_{2.5}$	1.44	0.72
CU AMS at SOAS CTR PM_{10}	0.93	0.47
AMS on SEAC ⁴ RS aircraft (RMA regression) PM_{10}	1.21	0.60
SEARCH (five site mean) $\text{PM}_{2.5}$	1.62	0.81

Table S7: Average concentration of ammonia at the SOAS Centreville site from 1 June 2013 to 15 July 2013. ppb to $\mu\text{g m}^{-3}$ conversions assume 303.15 K (1 ppb = $0.68 \mu\text{g m}^{-3}$).

Instrument	Number of Hourly Aggregated Observations	Ammonia (ppb)	Ammonia ($\mu\text{g m}^{-3}$)	Ratio of Means: $\text{NH}_4^+/\text{NH}_x$
SEARCH CTR	915	0.38	0.26	0.68
MARGA (Allen et al., 2015)	948	0.75	0.51	0.55
CIMS (You et al., 2014)	799	0.52	0.36	NA
URG Corporation Ambient Ion Monitor (AIM) 9000-D	370	0.85	0.58	0.50

Table S8: Mean C^* accounting for the effects of temperature and ideality in CLLPS and EQLB and for pure the species at 298.15 K (Adj Psat, adjusted vapor pressure calculations). For AIOMFAC calculations, C^* follows equation 4. Thus, for a system with two liquid phases (α and β) in the particle (PM), the following results:

$$C_i^* = \frac{P_i^{sat} \gamma_i^\alpha (\sum_k C_k^{PM})}{RT (\sum_k C_k^\alpha / M_k)} \left(\frac{C_i^\alpha}{C_i^\alpha + C_i^\beta} \right) \quad (S2)$$

where P_i^{sat} is the pure species vapor pressure at temperature T, γ_i^α is the mole-fraction based activity coefficient for species i in the α phase, C_i^α is the mass concentration of species i in the α phase, C_i^β is the mass concentration of species i in the β phase, M_k is the molecular mass of species k , and the summations are over all PM species (water, organic compounds, and inorganic compounds). The C_i^* could be defined analogously for the β phase. For one liquid phase, the equation reduces to:

$$C_i^* = \frac{P_i^{sat} \gamma_i M_{PM}}{RT} \quad (S3)$$

where the effective PM molecular mass (M_{PM}) is:

$$M_{PM} = \frac{\sum_k C_k^{PM}}{\sum_k C_k^\alpha / M_k} \quad (S4)$$

species	CLLPS C^* ($\mu\text{g m}^{-3}$)	EQLB C^* ($\mu\text{g m}^{-3}$)	Pure Species C^* ($\mu\text{g m}^{-3}$)	Ratio EQLB C^* / CLLPS C^*	Ratio EQLB C^* / Pure C^*
2-methyltetrol	6.0	3.7	7.7	0.62	0.47
pinic acid	13	16	5.1	1.19	3.09
C ₅ -alkene triol	22	17	14	0.78	1.19
2-methylglyceric acid	43	22	69	0.50	0.31
levoglucosan	1.6	1.4	4	0.90	0.35
pinonic acid	2.0E+04	3.1E+04	1.7E+03	1.55	18.7
hydroxyglutaric acid	0.85	0.60	2	0.71	0.29

Table S9: Mean activity coefficients predicted by AIOMFAC (mole-fraction based) for semivolatile organics (Adj Psat calculations). The β phase was organic-rich in both CLLPS and EQLB calculations.

species	γ CLLPS β phase	γ EQLB β phase	γ EQLB α phase	Ratio: γ_β EQLB/ γ_β CLLPS
2-methyltetrol	0.63	0.77	4.7E+03	1.23
pinic acid	5.22	16.21	1.4E+09	3.10
C ₅ -alkene triol	1.37	2.04	9.3E+04	1.49
2-methylglyceric acid	0.49	0.48	23	0.97
levoglucosan	0.42	1.02	1.4E+05	2.45
pinonic acid	26.60	121.31	1.3E+10	4.56
hydroxyglutaric acid	0.36	0.96	290	2.63

Table S.10: Comparison of CMAQ predicted aerosol species concentrations and CSN and SEARCH network observations in the Southeast U.S. NOAA climate region.

Species	Network	n	Mean O_i	Mean O_i	Mean M_i	Mean M_i	Mean $\frac{M_i}{O_i}$	Mean $\frac{M_i}{O_i}$	r^2	MB	ME	NMB	NME	FB	FE	IofA	RMSE
			$\frac{\mu\text{g}}{\text{m}^3}$	$\frac{\mu\text{mol}}{\text{m}^3}$	$\frac{\mu\text{g}}{\text{m}^3}$	$\frac{\mu\text{mol}}{\text{m}^3}$	$\frac{\mu\text{g}}{\text{m}^3}$	$\frac{\mu\text{mol}}{\text{m}^3}$		$\frac{\mu\text{g}}{\text{m}^3}$	$\frac{\mu\text{g}}{\text{m}^3}$	%	%	%	%		$\frac{\mu\text{g}}{\text{m}^3}$
		=							=						=		
SO ₄ ²⁻	CSN	225	1.53	0.0159	1.61	0.0168	1.1	0.48	0.07	0.46	5	30	4	32	0.82	0.59	
SO ₄ ²⁻	SEARCH	97	1.77	0.0184	1.56	0.0163	0.9	0.49	-0.22	0.50	-12	28	-16	35	0.82	0.65	
NH ₄ ⁺	CSN	225	0.27	0.0147	0.40	0.0221	1.5	0.50	0.13	0.20	50	75	44	75	0.79	0.26	
NH ₄ ⁺	SEARCH	95	0.54	0.0301	0.38	0.0211	0.7	0.37	-0.16	0.26	-30	47	-57	71	0.71	0.31	
Na ⁺	CSN	224	0.05	0.0024	0.12	0.0053	2.3	0.36	0.07	0.08	126	146	72	88	0.62	0.12	
Na ⁺	SEARCH	93	0.05	0.0020	0.12	0.0053	2.6	0.49	0.08	0.08	164	168	74	80	0.49	0.14	
Ca ²⁺	CSN	224	0.03	0.0007	0.13	0.0032	4.8	0.45	0.10	0.11	378	387	118	122	0.36	0.17	
Ca ²⁺	SEARCH	201	0.03	0.0007	0.16	0.0040	5.9	0.67	0.13	0.13	490	490	118	118	0.23	0.24	
Mg ²⁺	CSN	224	0.00	0.0002	0.02	0.0007	4.1	0.04	0.01	0.02	308	379	76	101	0.38	0.02	
K ⁺	CSN	224	0.06	0.0016	0.17	0.0042	2.7	0.09	0.10	0.12	166	186	57	77	0.24	0.18	
K ⁺	SEARCH	201	0.06	0.0015	0.18	0.0045	3.1	0.05	0.12	0.13	207	228	61	78	0.18	0.22	
Cl ⁻	CSN	224	0.02	0.0005	0.03	0.0009	1.6	0.09	0.01	0.03	61	148	17	97	0.46	0.07	
NO ₃ ⁻	CSN	225	0.31	0.0049	0.27	0.0044	0.9	0.07	-0.04	0.22	-12	73	-48	84	0.43	0.35	
NO ₃ ⁻	SEARCH	97	0.05	0.0008	0.30	0.0048	6.0	0.18	0.25	0.27	497	542	48	110	0.10	0.62	

For a given set of n model predictions, $\{M_i\}$, and observations, $\{O_i\}$:

$$\text{MB, Mean bias} = \frac{1}{n} \sum_i^n (M_i - O_i)$$

$$\text{ME, Mean error} = \frac{1}{n} \sum_i^n |M_i - O_i|$$

$$\text{NMB, Normalized mean bias} = \frac{\sum_i^n (M_i - O_i)}{\sum_i^n O_i} \times 100\%$$

$$\text{NME, Normalized mean error} = \frac{\sum_i^n |M_i - O_i|}{\sum_i^n O_i} \times 100\%$$

$$\text{FB, Fractional bias} = \frac{1}{n} \frac{\sum_i^n (M_i - O_i)}{\sum_i^n (M_i + O_i)/2} \times 100\%$$

$$\text{FE, Fractional error} = \frac{1}{n} \frac{\sum_i^n |M_i - O_i|}{\sum_i^n (M_i + O_i)/2} \times 100\%$$

$$\text{IofA, Index of agreement} = 1 - \frac{\sum_i^n (O_i - M_i)^2}{\sum_i^n (|M_i - O_i| + |O_i - O_i|)^2}$$

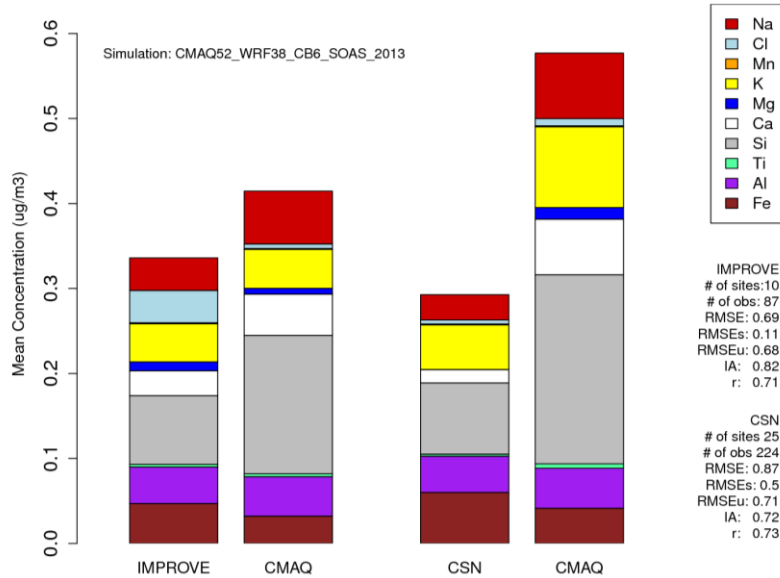
$$\text{RMSE, Root mean square error} = \sqrt{\frac{\sum_i^n (M_i - O_i)^2}{n}}$$

Formatted: Space After: 6 pt, Line spacing: single

Formatted: Font: 10 pt

Figure S1: Observed (CSN, IMPROVE) and modeled (CMAQ) ions for June 1, 2013 to July 15, 2013.

(a) Major cations and anions for the Southeast US, NOAA Climate Region (FL, GA, SC, NA, VA)



(b) Major cations and anions for the Central US NOAA Climate Region

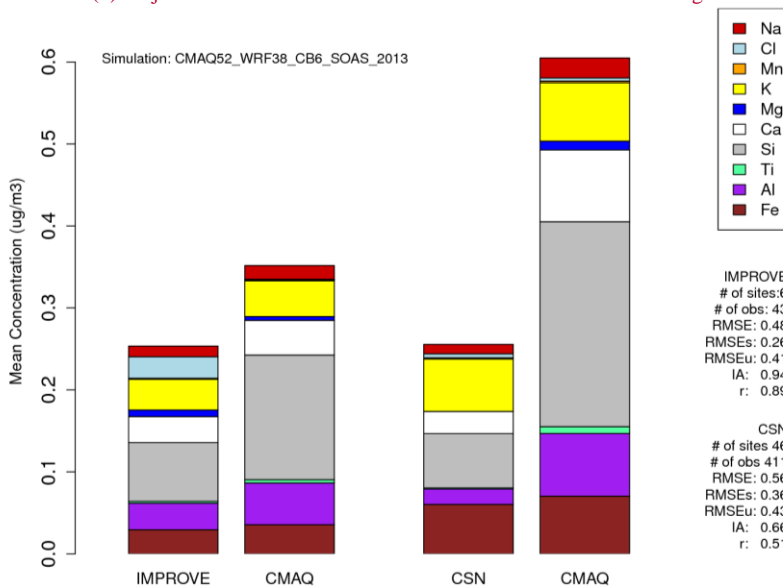
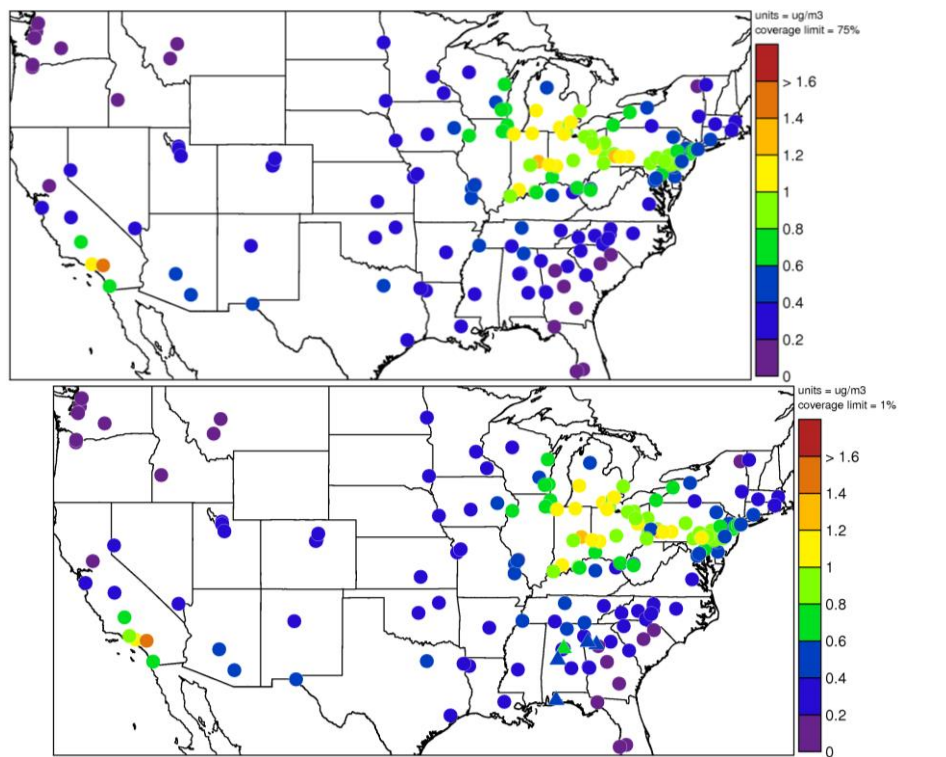


Figure S2: Observed (CSN-circle, SEARCH-triangle) and modeled (CMAQ) ammonium for June 1, 2013 to July 15, 2013. Ammonium is not measured by the IMPROVE network.

(a) Observed Ammonium ($\mu\text{g m}^{-3}$)



(b) Modeled - Observed Ammonium ($\mu\text{g m}^{-3}$)

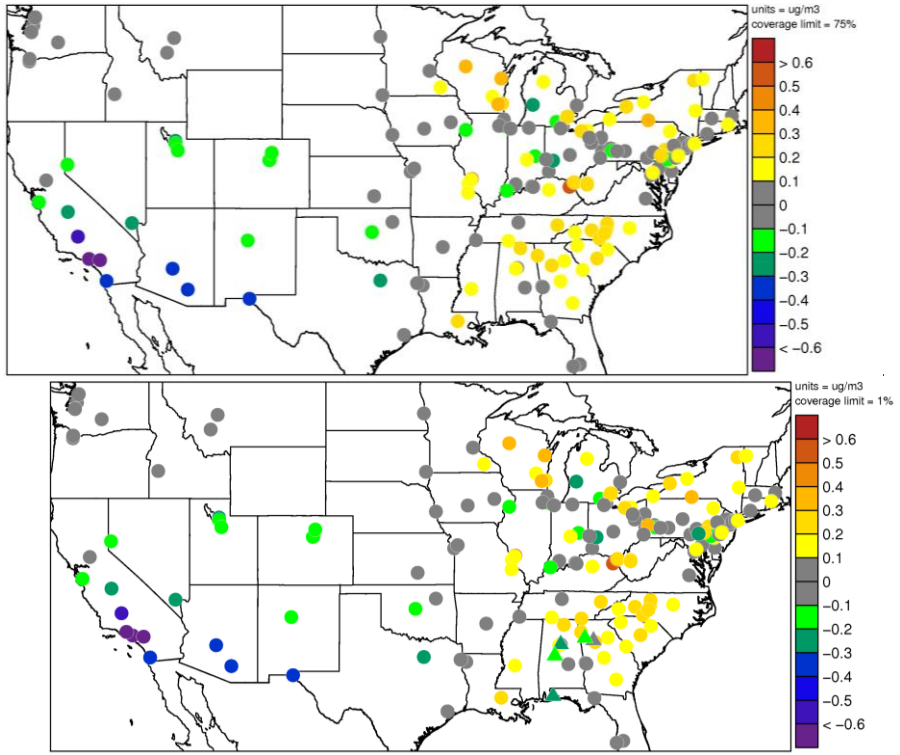
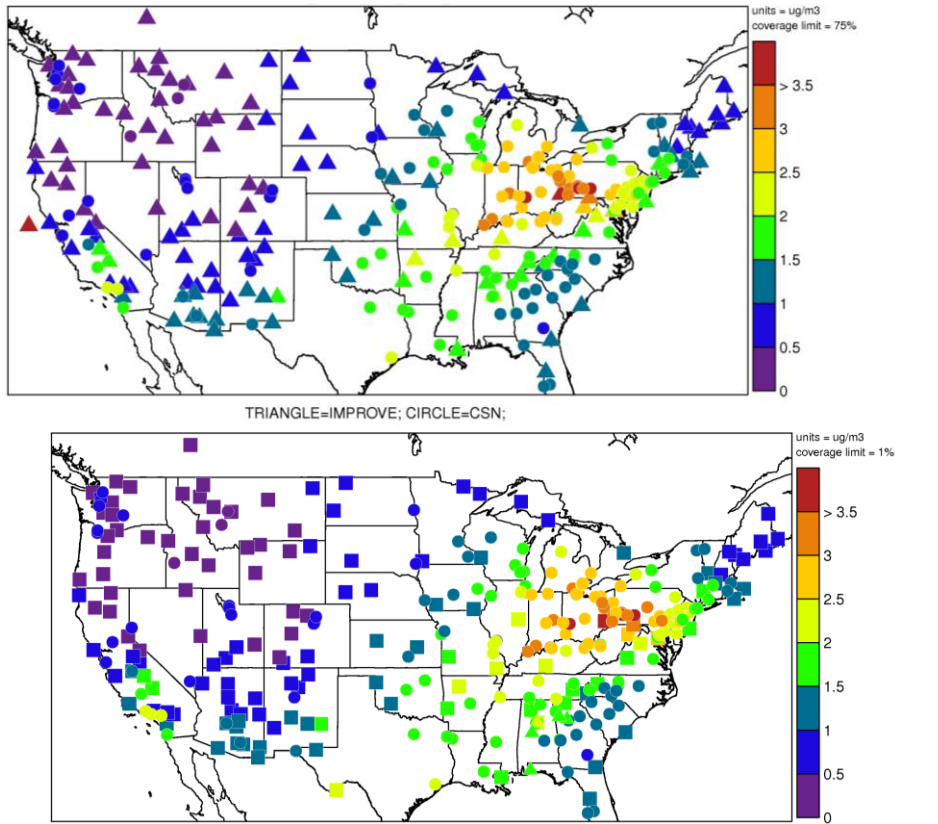


Figure S3: Observed (IMPROVE-square, CSN-circle, SEARCH-triangle) and modeled (CMAQ) sulfate for June 1, 2013 to July 15, 2013.

(a) Observed sulfate ($\mu\text{g m}^{-3}$)



(b) Modeled - Observed sulfate ($\mu\text{g m}^{-3}$)

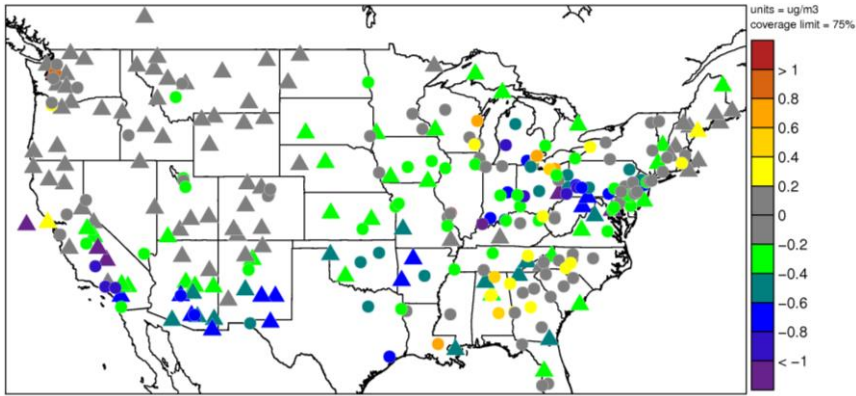
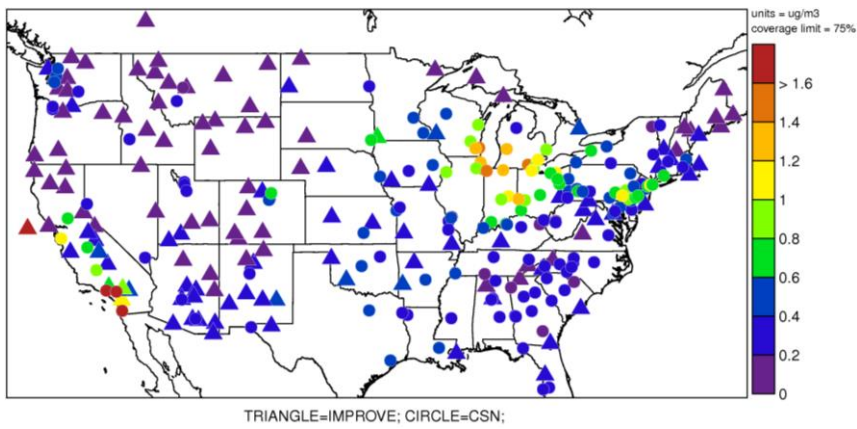


Figure S4: Observed (IMPROVE, CSN) and modeled (CMAQ) nitrate for June 1, 2013 to July 15, 2013.

(a) Observed Nitrate ($\mu\text{g m}^{-3}$)



(b) Modeled — Observed Nitrate ($\mu\text{g m}^{-3}$)

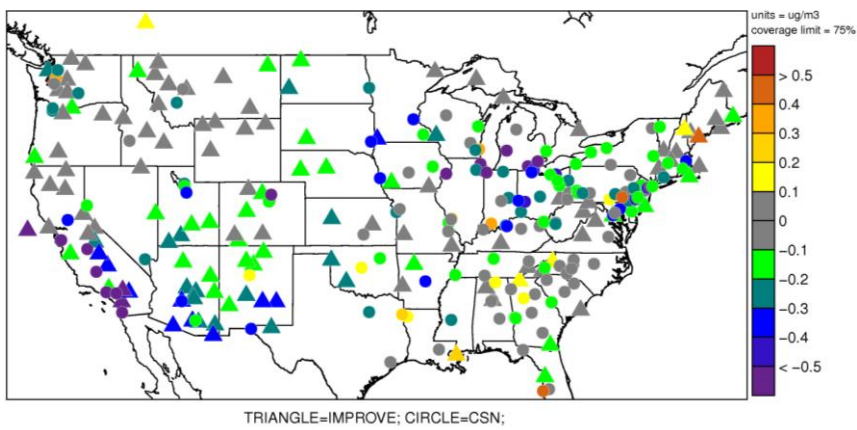


Figure S5: PM_{2.5} Stacked Bar Plot for the (a) Southeast and (b) Central US NOAA Climate Region predicted by CMAQ and measured by CSN June 1, 2013 – July 15, 2013. Soil is calculated using the IMPROVE equation (Soil = (2.20 × Al) + (2.49 × Si) + (1.63 × Ca) + (2.42 × Fe) + (1.94 × Ti); http://vista.cira.colostate.edu/improve/publications/graylit/023_SoilEquation/Soil_Eq_Evaluation.pdf); NCOM in non-carbon organic matter (total organic matter minus organic carbon).

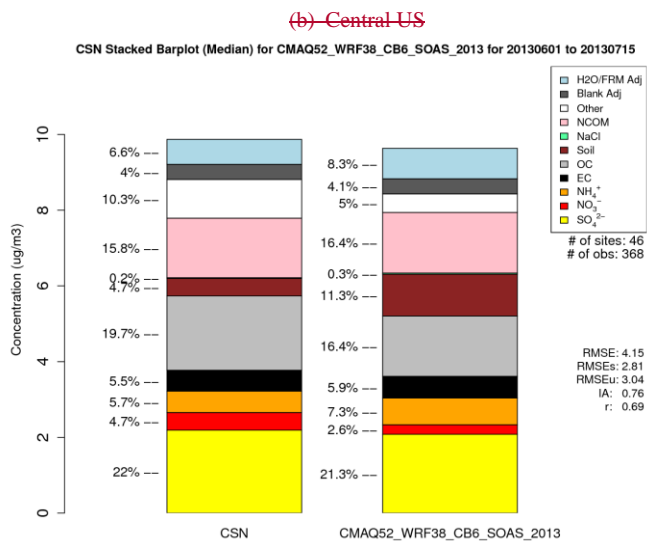
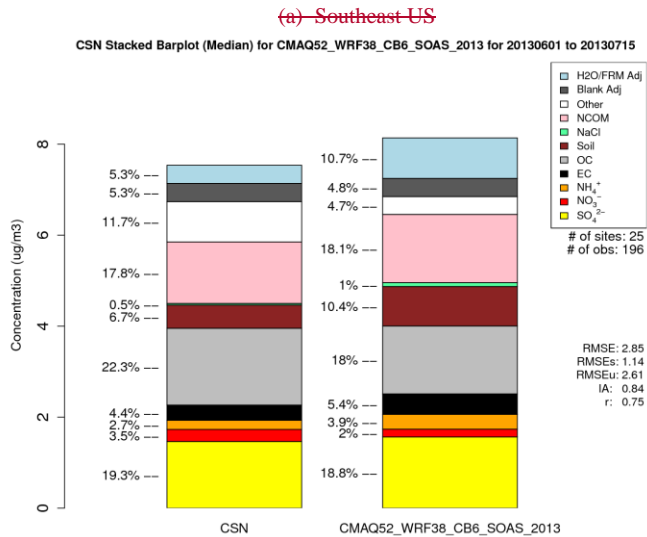


Figure S6

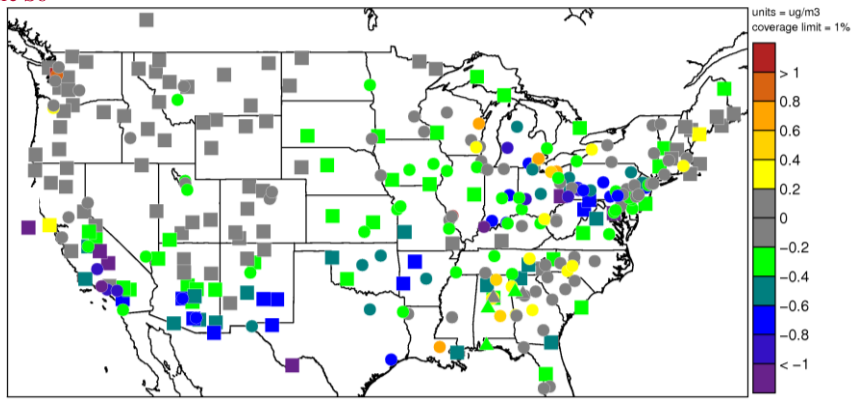


Figure S4: Modeled vs Observed (CSN) Molar Ratio of (a) ammonium to 2 × sulfate and (b) cations to anions (2 × calcium + potassium + sodium + ammonium + 2 × magnesium)/(2 × sulfate + nitrate + chloride).

Formatted: Space After: 8 pt, Line spacing: Multiple 1.08 li

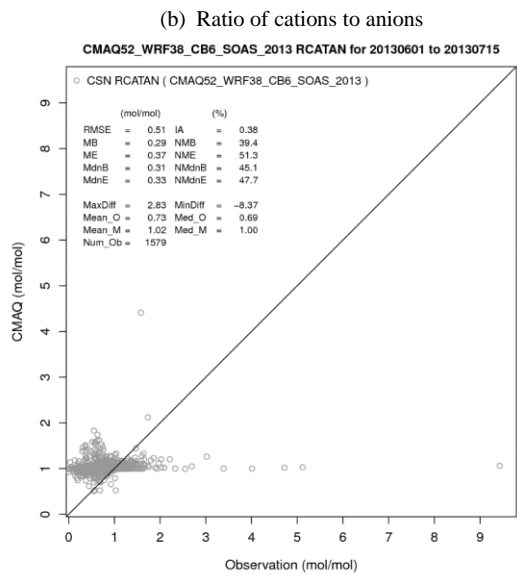
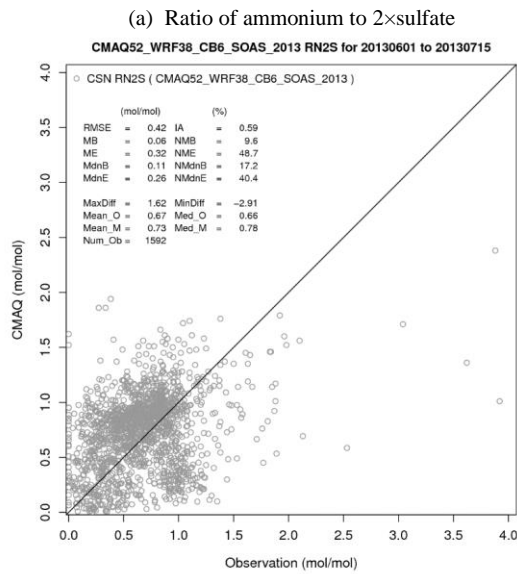


Figure S7S5: (a) Observed (Ammonia monitoring Network, AMoN), (b) CMAQ simulated, and (c) model bias in gas-phase ammonia concentrations June 1, 2013- July 15, 2013.

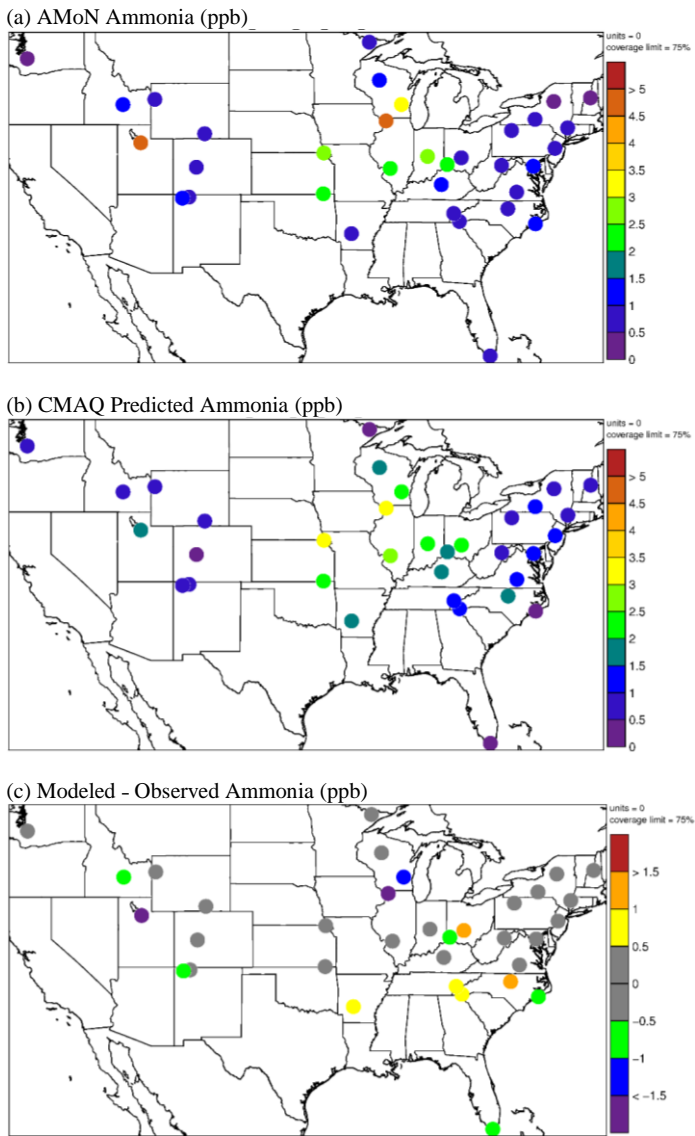


Figure S8S6: Observed and CMAQ predicted inorganic species at SOAS Centreville site.

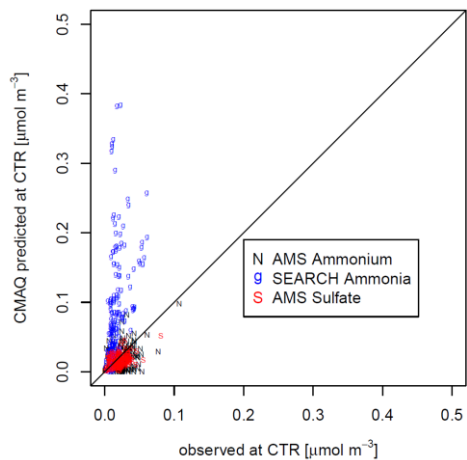


Figure S9S7: Liquid-liquid phase separation as a function of hour of day predicted by AIOMFAC for the ammonium-sodium-sulfate-nitrate-chloride and organic surrogates system. Shown is the percentage of the time a phase separation was predicted in a certain hour-of-day bin. For reference, the oxygen-to-carbon ratio based separation relative humidity (SRH) as parameterized by You et al. (2013) is shown in blue.

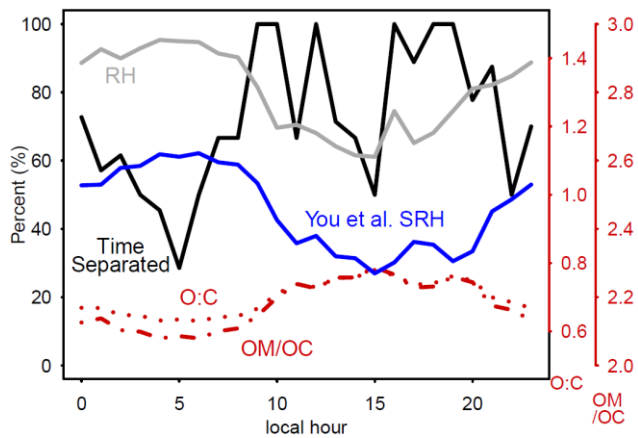
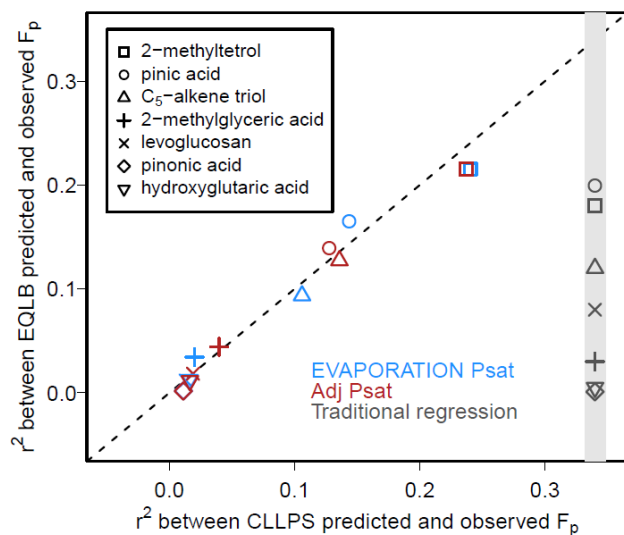


Figure S10S8: r^2 (square of Pearson's r) between model predicted and observed F_p for each explicit semivolatile species. The x-axis location is arbitrary for the Traditional regression (equation S1). r^2 does not exceed 0.25 for any species or method.



References

- Allen, H. M., Draper, D. C., Ayres, B. R., Ault, A., Bondy, A., Takahama, S., Modini, R. L., Baumann, K., Edgerton, E., Knote, C., Laskin, A., Wang, B., and Fry, J. L.: Influence of crustal dust and sea spray supermicron particle concentrations and acidity on inorganic NO_3^- aerosol during the 2013 Southern Oxidant and Aerosol Study, *Atmos. Chem. Phys.*, 15, 10669-10685, doi: 10.5194/acp-15-10669-2015, 2015.
- Compernelle, S., Ceulemans, K., and Müller, J. F.: EVAPORATION: a new vapour pressure estimation method for organic molecules including non-additivity and intramolecular interactions, *Atmos. Chem. Phys.*, 11, 9431-9450, doi: 10.5194/acp-11-9431-2011, 2011.
- Hu, W. W., Campuzano-Jost, P., Palm, B. B., Day, D. A., Ortega, A. M., Hayes, P. L., Krechmer, J. E., Chen, Q., Kuwata, M., Liu, Y. J., de Sá, S. S., McKinney, K., Martin, S. T., Hu, M., Budisulistiorini, S. H., Riva, M., Surratt, J. D., St. Clair, J. M., Isaacman-Van Wertz, G., Yee, L. D., Goldstein, A. H., Carbone, S., Brito, J., Artaxo, P., de Gouw, J. A., Koss, A., Wisthaler, A., Mikoviny, T., Karl, T., Kaser, L., Jud, W., Hansel, A., Docherty, K. S., Alexander, M. L., Robinson, N. H., Coe, H., Allan, J. D., Canagaratna, M. R., Paulot, F., and Jimenez, J. L.: Characterization of a real-time tracer for isoprene epoxydiols-derived secondary organic aerosol (IEPOX-SOA) from aerosol mass spectrometer measurements, *Atmos. Chem. Phys.*, 15, 11807-11833, doi: 10.5194/acp-15-11807-2015, 2015.
- Myrdal, P. B., and Yalkowsky, S. H.: Estimating pure component vapor pressures of complex organic molecules, *Ind. Eng. Chem. Res.*, 36, 2494-2499, doi: 10.1021/ie950242l, 1997.
- Nannoolal, Y., Rarey, J., Ramjugernath, D., and Cordes, W.: Estimation of pure component properties: Part 1. Estimation of the normal boiling point of non-electrolyte organic compounds via group contributions and group interactions, *Fluid Phase Equilib.*, 226, 45-63, doi: 10.1016/j.fluid.2004.09.001, 2004.
- Nannoolal, Y., Rarey, J., and Ramjugernath, D.: Estimation of pure component properties: Part 3. Estimation of the vapor pressure of non-electrolyte organic compounds via group contributions and group interactions, *Fluid Phase Equilib.*, 269, 117-133, doi: 10.1016/j.fluid.2008.04.020, 2008.
- Pankow, J. F., and Asher, W. E.: SIMPOL.1: a simple group contribution method for predicting vapor pressures and enthalpies of vaporization of multifunctional organic compounds, *Atmos. Chem. Phys.*, 8, 2773-2796, doi: 10.5194/acp-8-2773-2008, 2008.
- Silvern, R. F., Jacob, D. J., Kim, P. S., Marais, E. A., Turner, J. R., Campuzano-Jost, P., and Jimenez, J. L.: Inconsistency of ammonium-sulfate aerosol ratios with thermodynamic models in the eastern US: a possible role of organic aerosol, *Atmos. Chem. Phys.*, 17, 5107-5118, doi: 10.5194/acp-17-5107-2017, 2017.
- Topping, D., Barley, M., Bane, M. K., Higham, N., Aumont, B., Dingle, N., and McFiggans, G.: UManSysProp v1.0: an online and open-source facility for molecular property prediction and atmospheric aerosol calculations, *Geosci. Model Dev.*, 9, 899-914, doi: 10.5194/gmd-9-899-2016, 2016.
- Xu, L., Guo, H., Boyd, C. M., Klein, M., Bougiatioti, A., Cerully, K. M., Hite, J. R., Isaacman-VanWertz, G., Kreisberg, N. M., Knote, C., Olson, K., Koss, A., Goldstein, A. H., Hering, S. V., de Gouw, J., Baumann, K., Lee, S.-H., Nenes, A., Weber, R. J., and Ng, N. L.: Effects of anthropogenic emissions on aerosol formation from isoprene and monoterpenes in the southeastern United States, *P. Natl. Acad. Sci. USA*, 112, 37-42, doi: 10.1073/pnas.1417609112, 2015a.

Xu, L., Suresh, S., Guo, H., Weber, R. J., and Ng, N. L.: Aerosol characterization over the southeastern United States using high-resolution aerosol mass spectrometry: spatial and seasonal variation of aerosol composition and sources with a focus on organic nitrates, *Atmos. Chem. Phys.*, 15, 7307–7336, doi:10.5194/acp-15-7307-2015, 2015b.

You, Y., Renbaum-Wolff, L., and Bertram, A. K.: Liquid-liquid phase separation in particles containing organics mixed with ammonium sulfate, ammonium bisulfate, ammonium nitrate or sodium chloride, *Atmos. Chem. Phys.*, 13, 11723-11734, doi: 10.5194/acp-13-11723-2013, 2013.

You, Y., Kanawade, V. P., de Gouw, J. A., Guenther, A. B., Madronich, S., Sierra-Hernández, M. R., Lawler, M., Smith, J. N., Takahama, S., Ruggeri, G., Koss, A., Olson, K., Baumann, K., Weber, R. J., Nenes, A., Guo, H., Edgerton, E. S., Porcelli, L., Brune, W. H., Goldstein, A. H., and Lee, S. H.: Atmospheric amines and ammonia measured with a chemical ionization mass spectrometer (CIMS), *Atmos. Chem. Phys.*, 14, 12181-12194, doi: 10.5194/acp-14-12181-2014, 2014.

Zuend, A., and Seinfeld, J. H.: Modeling the gas-particle partitioning of secondary organic aerosol: the importance of liquid-liquid phase separation, *Atmos. Chem. Phys.*, 12, 3857-3882, doi: 10.5194/acp-12-3857-2012, 2012.